

## Review of experimental sorption studies of CO<sub>2</sub> and CH<sub>4</sub> in shales

Isaac Klewiah<sup>a,\*</sup>, Dhruvit S. Berawala<sup>b,c</sup>, Hans Christian Alexander Walker<sup>a</sup>,  
Pål Ø. Andersen<sup>a,b,c</sup>, Paul H. Nadeau<sup>a</sup>

<sup>a</sup> Department of Energy Resources, University of Stavanger, 4036, Norway

<sup>b</sup> Department of Energy and Petroleum Engineering, University of Stavanger, 4036, Norway

<sup>c</sup> The National IOR Centre of Norway, University of Stavanger, 4036, Norway

### ARTICLE INFO

#### Keywords:

Gas sorption  
Shale reservoirs  
Enhanced gas recovery  
Carbon storage and sequestration  
Adsorption isotherms

### ABSTRACT

In recent years CO<sub>2</sub> injection in shale has been investigated with aim to enhance shale gas recovery (ESGR) and permanently sequester CO<sub>2</sub>. This paper reviews the state of research on CH<sub>4</sub> and CO<sub>2</sub> sorption in shale. We present the interaction of CO<sub>2</sub> and CH<sub>4</sub> with shale rocks and discuss the dependence of gas sorption on shale properties including organic matter content, kerogen type, mineralogy, moisture and temperature as well as shale selectivity for either species. Dynamic CO<sub>2</sub>-CH<sub>4</sub> exchange studies are also summarized together with the geochemical and mechanical impact of gas sorption in shales. We note that most experimental work is still performed on crushed samples rather than whole cores. Also, CO<sub>2</sub> is preferentially adsorbed over CH<sub>4</sub> when both species co-exist in shale. Both gases are in supercritical state at typical reservoir conditions. Especially CO<sub>2</sub> adsorption is not well described by standard isotherm models in this state.

### 1. Introduction

Natural gas production from shales has become exceedingly important in satisfying the ever-growing global energy demands. This unconventional hydrocarbon system is globally abundant, with large technically recoverable resources reported in China (1115 tcf), Argentina (802 tcf), US (665 tcf) and Canada (573 tcf) (EIA, 2013). Commercial exploitation of shale resources has led to a shale energy revolution in the last decade. Successful implementation of large-scale horizontal drilling and hydraulic fracturing techniques (Wang and Krupnick, 2015) made this possible and is attributed to collaborative efforts by the natural gas industry (notably Mitchell Energy) and the U.S. Department of Energy (DOE) from the 1980s.

A typical gas shale system is a blend of organic-rich deposition and complex mineralogy that forms a fine-grained clastic sedimentary rock with a unique geological framework where the shale independently exists as source, trap and reservoir. Common types are black shale (rich in organic matter), carbonaceous shale (rich in organic matter that has been carbonized), siliceous shale (high amount of quartz), iron shale (having some fractions of iron oxides, hydroxides, etc.) and oil shale (containing a certain amount of bitumen/asphalt) (Curtis, 2002; Wang et al., 2012). Shale rocks have grains with sizes often less than 62.5 μm with pore body and throat sizes ranging from micropores (<0.1 μm) to

nanopores (nm) (Sondergeld et al., 2010; Chen et al., 2019). The pores in shale are associated with both organic and mineral matter (Tang et al., 2016). Loucks et al. (2012) presented a descriptive classification of shale matrix-related pore types, differentiating between interparticle (located between particles and crystals) and intraparticle (existing within particles) pores affiliated with the mineral matrix and intraparticle organic matter pores. The hydrocarbons are generated in-situ through biogenic and thermogenic processes (Krooss et al., 1995) and are stored in three different states; as free compressed gas in the open pores and microcracks; as adsorbed gas on the nanopore/micropore inner surfaces of shale organic and inorganic components; or as solution gas absorbed within the solid organic matter and connate water (Bustin et al., 2008). Natural gas in shale is predominantly methane (>94%) with minor fractions of ethane, propane and butane plus traces of CO<sub>2</sub> and N<sub>2</sub> (Kalkreuth et al., 2013).

Low intrinsic matrix permeability (e.g. 0.1 μD for Huron shales (Soeder, 1988)) coupled with structural heterogeneity and complex pore networks complicates fluid transport and storage within the formation and poses tremendous challenges to technical evaluation and effective development. Although current technological advancements in horizontal drilling and fluid fracturing have contributed to primary production, only 5–10% of the original gas in place (OGIP) is estimated to be recovered economically (Rassenfoss, 2017) leaving a high potential

\* Corresponding author.

E-mail addresses: [isaacklewiah@gmail.com](mailto:isaacklewiah@gmail.com), [isaacklewiah@yahoo.com](mailto:isaacklewiah@yahoo.com) (I. Klewiah).

<https://doi.org/10.1016/j.jngse.2019.103045>

Received 3 June 2019; Received in revised form 26 October 2019; Accepted 26 October 2019

Available online 31 October 2019

1875-5100/© 2019 The Authors. Published by Elsevier B.V. This is an open access article under the CC BY license (<http://creativecommons.org/licenses/by/4.0/>).

for enhanced recovery methods. The gas stored by sorption in the shale matrix is estimated to account for 20–80% of the total gas fraction (Lane et al., 1989; Bruner and Smosna, 2011; Edwards et al., 2015). Desorption is triggered by pressure reduction and/or presence of a favourably adsorbing gas.

Experimental results have shown that shales have greater adsorption affinity for CO<sub>2</sub> than CH<sub>4</sub> (Weniger et al., 2010; Heller and Zoback, 2014). CO<sub>2</sub> is also favourably adsorbed over CH<sub>4</sub> when both gas species co-exist within the shale (Pino et al., 2014; Cancino et al., 2017; Ma et al., 2018). A huge potential for enhanced shale gas recovery (ESGR) is therefore feasible through injection of CO<sub>2</sub> (Blok et al., 1997; Oldenburg et al., 2001) which can stimulate the desorption of pre-adsorbed methane through an in-situ molecular swapping mechanism at the sorption sites, releasing the otherwise trapped methane into the porous system to increase the rate and volume of CH<sub>4</sub> recovered (Regan, 2007). This technique is referred to as CO<sub>2</sub> enhanced shale gas recovery, CO<sub>2</sub>-ESGR and is considered a viable means for simultaneous CO<sub>2</sub> storage in the shale formations with recent reviews provided by Liu et al. (2019) and Rani et al. (2019). This concept of CO<sub>2</sub> utilization in shales is illustrated in Fig. 1. Godec et al. (2013) demonstrated through simulation that at optimal operational conditions, 7% incremental CH<sub>4</sub> production could be obtained through CO<sub>2</sub> injection in the Marcellus Shale in Eastern United States. They estimated 12 trillion cubic meters of methane to be technically recoverable with an associated storage of 55 billion tonnes of CO<sub>2</sub>. Khosrokhavar (2015) demonstrated that for an approximate storage of 12 kg of CO<sub>2</sub> in a characteristic gas shale system, 1 kg of CH<sub>4</sub> can be produced and yield 55 MJ energy while spending 12 MJ energy for compression. They noted that the energy gain was still substantial when accounting for CO<sub>2</sub> capture and storage (CCS) as quantified by Iijima et al. (2011). Logistically, in most cases, a surface gas pipeline distribution network could easily be modified to transport CO<sub>2</sub> to the wellhead whereas the cost of CO<sub>2</sub> injection into the subsurface formation is drastically minimized by repurposing the available well infrastructure to accommodate CO<sub>2</sub> injection (Tao et al., 2014).

## 2. Objectives and scope

The mechanisms in the CO<sub>2</sub>-ESGR system are complex, many and coupled. Key parameters include storage capacity and form of CH<sub>4</sub> and CO<sub>2</sub>, CO<sub>2</sub>-CH<sub>4</sub> competitive sorption, isotherms and diffusion; chemical and geomechanical impact of gas sorption and desorption (shrinkage and swelling); CO<sub>2</sub> injectivity and trapping integrity. Many of these parameters are interrelated, further coupled to the intricate petrographic nature of shales, inherent structural heterogeneities and

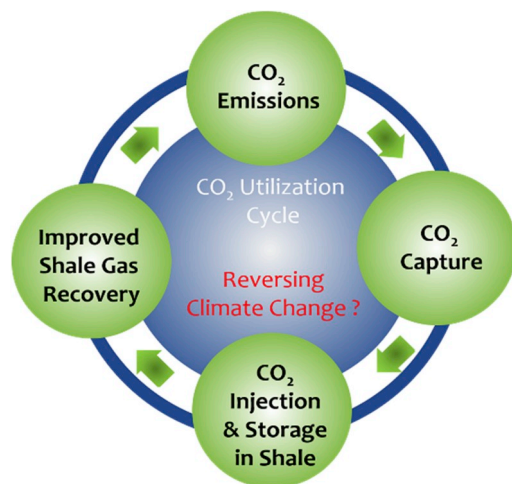


Fig. 1. Concept of CO<sub>2</sub> capture and utilization for enhanced shale gas recovery and carbon sequestration.

variation of pressure and temperature. To limit our scope, our objectives are:

- Evaluate the state of experimental findings regarding gas sorption in shales
- Determine gaps in experimental research that should be addressed

Detailed theories of adsorption phenomena, experimental tools and associated uncertainties are not specifically addressed. For such aspects we refer to Polanyi (1932); Steele (1974); Sing et al. (1985); Sircar (1985); Malbrunot et al. (1997); Neimark and Ravikovitch (1997); Cavenati et al. (2004); Ross and Bustin (2007b); Busch and Gensterblum (2011); Rudzinski and Everett (2012).

The paper is organized as follows:

- Mechanisms for gas sorption on shale and relevant isotherm models (3.1), definition of useful thermodynamical parameters (3.2) and adsorption behavior of individual gas species (3.3).
- Dependence of CO<sub>2</sub> and CH<sub>4</sub> sorption capacity on shale physico-chemical parameters such as organic matter (4.1), thermal maturity (4.2), kerogen type (4.3), inorganic content (4.4), moisture content (4.5) and temperature (4.6).
- CO<sub>2</sub> versus CH<sub>4</sub> comparative adsorption capacity on shale (5.0).
- Recent advances in experimental work related to dynamic CO<sub>2</sub>-CH<sub>4</sub> exchange and transport in gas shales (5.1).
- Experimental work on geomechanical (5.2) and geochemical (5.3) impact of gas adsorption-desorption on shale.
- Brief discussion of presented findings
- Conclusions and recommendations

## 3. Gas sorption on shale

Gas sorption in shales is a comprehensive term for surface accumulation onto organic and mineral surfaces (adsorption), absorption (soaking or imbibition) into organic molecular (kerogen) openings and capillary condensation within the pores. Gas adsorption on shale matrix surfaces is governed by physisorption (Brunauer et al., 1940). This is a result of weak van der Waals and electrostatic interaction forces between the gas molecules (adsorbates) and the shale surface (the adsorbent). This is enhanced by the abundant nano-microscale pores (Nelson, 2009) that provide a large internal surface area and restrictions that force the fluid-solid phases closely enough for weak dipole-dipole interaction to occur and bind the gas species to the shale surfaces. Physisorption is deemed reversible, due to the absence of adsorbate-adsorbent covalent bonds.

Sorption of CO<sub>2</sub> or CH<sub>4</sub> onto shale matrix is frequently examined in the laboratory by construction of sorption isotherms, which involves measuring the uptake or release of either gas species on a shale sample at controlled temperature and pressure conditions. The measured sorption is a combination of adsorption, absorption or capillary condensation which individually are difficult to distinguish. Although these mechanisms are characteristically different, the net result is a storage of gas molecules in a denser phase relative to the bulk (free gas) phase in the open pores (Ross and Bustin, 2009). The experimental procedures to measure sorption vary but can be categorized into mass-based or volumetric-based. In the mass-based method the change in sample mass associated with adsorption at each fixed pressure and temperature condition is measured with a microbalance of high accuracy. The volumetric technique is based on Boyle's law, where the adsorption isotherms are constructed by computing the amount of adsorbed gas using the real gas equation, which accounts for the gas compressibility factor at each equilibrium pressure (Heller and Zoback, 2014). The former approach is limited to the use of very small sample sizes whereas the latter can satisfactorily accommodate different sample sizes.

The reviewed literature depicts tremendous challenge with performing experimental flow-through tests due to the characteristically

ultra-low permeability of shale rocks. Hence most experimental evaluations of gas sorption have been conducted with crushed samples as opposed to whole cores. Likely sources of experimental errors and uncertainties in these tests are discussed by Fraissard and Conner (1997); Busch and Gensterblum (2011). In general, high-pressure isotherm experiments determine sorption capacity, whereas structural properties (e.g. specific surface area, pore size distribution, nano-, micro- or mesopore volumes) are evaluated via low-pressure (<1 MPa) sorption tests.

### 3.1. Gas sorption isotherm models

The quantity obtained in laboratory measurements is excess sorption (also called Gibbs sorption) (Burwell, 1977). It is the amount sorbed in excess of the molecular gas volume that would be present in the sample if the sorbed-phase volume were filled with bulk gas (Heller and Zoback, 2014). The total or absolute amount sorbed is computed by mathematical modelling, before fitting the data to one of many available mathematical isotherm models (e.g. Henry, Langmuir, BET, DR, Pore-filling). It is suspected that adsorption occurs as a monolayer at low pressures and as multilayers at higher pressures. The Langmuir model, which assumes monolayer adsorption, is widely reported as the most suitable fit for gas adsorption on shales (Lu et al., 1995; Nuttal et al., 2005; Chalmers and Bustin, 2008; Ji et al., 2012; Yuan et al., 2014; Hong et al., 2016).

This isotherm is reasonably simple and can be fit to data with a two-parameter equation (Langmuir, 1916, 1918) given as:

$$V_p = \frac{V_L P}{P_L + P} \quad (1)$$

where  $V_p$  is the adsorbed volume at pressure  $P$ ,  $V_L$  is the Langmuir volume (total adsorption volume at infinite pressure), and  $P_L$  is the Langmuir pressure (the pressure at which half the Langmuir volume is adsorbed). Some authors (e.g. Duan et al., 2016) have also found the BET model (which accounts for multilayer adsorption) as a satisfactory choice. Indeed, the acceptance of a single model for universal description of sorption in shales is still contended amongst researchers. A review by Tang et al. (2017) presents some widely used adsorption models with comparisons and distinctive applications. Besides revealing the adsorptive potential for a material, the magnitude and shape of the sorption isotherm suggests the relation between pore accessibility and pressure, information regarding adsorption/desorption, sorption capacity, rates, pore structure, as well as surface properties of the shale matrix. This is primarily because the physical sorption process is inextricably linked to the effects that the confined pore space exerts on the state and thermodynamic stability of the gas species held onto the nano-pores (Thommes, 2010).

### 3.2. Adsorption thermodynamics

Sorption isotherms are frequently employed as basis for applying thermodynamical principles to interpretation of adsorption phenomena. This often implies the computation of parameters such as adsorption energy, binding energy, activation energy or heat of adsorption. The latter has especially been applied in the evaluation of CH<sub>4</sub> and CO<sub>2</sub> adsorption on shales (Chikatamarla and Crosdale, 2001; Rexer et al., 2014; Xiong et al., 2017; Chen et al., 2019). The isosteric heat of adsorption indicates the strength of interaction between the adsorbent and adsorbate (in this case the shale surfaces and the gas species; greater values indicative of stronger adsorbate-adsorbent bonding). By classical definition, it reflects the energy evolved when one molecule of adsorbate is added to an adsorption system. It depends on the gas type, surface chemistry and pore structure. It is a strong function of adsorbate density and surface coverage. The heat of adsorption for CO<sub>2</sub> is reportedly greater than for CH<sub>4</sub> in gas shales; indicative of greater affinity of shale for CO<sub>2</sub> over methane (Luo et al., 2015; Duan et al., 2016). In

adsorption, activation energy is the minimum energy needed (to overcome the adsorbate-adsorbent repulsion) for the gas molecules to react/interact with adsorption sites in the shale rock formation. Also, when adsorbate (gas) molecules interact with surfaces of an adsorbent (i.e. shale, in this case), the adsorption energy ( $E_{ads}$ ) is defined as:

$$E_{ads} = E_{sys} - (E_{mol} + E_{surf}) \quad (2)$$

where  $E_{sys}$ ,  $E_{mol}$  and  $E_{surf}$  represents the energy of the total adsorbate-adsorbent system, the gas phase molecules and the shale surface respectively.  $E_{ads}$  also equals sum of the binding energy ( $E_b$ , characterizing the interaction between a single isolated gas molecule with the shale surface) and adsorbate stabilization energy ( $E_{inter-ad}$ ) which accounts for intermolecular interactions between the gas molecules (Bocquet et al., 2005)

$$E_{ads} = E_b + E_{inter-ad} \quad (3)$$

CO<sub>2</sub>, CH<sub>4</sub> adsorption is an exothermic process, making  $E_{ads}$  a negative variable. On the other hand, a negative (or positive) binding energy implies that the adsorption is favorable (or unfavorable) (Scaranto et al., 2011). The nature of these parameters, interrelationship and theoretical variance has been discussed by Saha and Chowdhury (2011) and Inglezakis and Zorpas (2012).

### 3.3. Single component sorption of CO<sub>2</sub> or CH<sub>4</sub> at reservoir conditions

The majority of shale formations have temperatures ranging from 96 to 122 °C, with pore pressures in the range of 15–25 MPa (Lu et al., 2016). The subsurface sorption phenomenon will most likely proceed as a supercritical adsorption-desorption process (Menon, 1968) since both CH<sub>4</sub> and CO<sub>2</sub> will typically exist in the supercritical state (CH<sub>4</sub>:  $T_{cr} = -82$  °C and  $P_{cr} = 4.64$  MPa; CO<sub>2</sub>:  $T_{cr} = 31$  °C and  $P_{cr} = 7.38$  MPa). A peculiar feature in adsorption isotherms of supercritical fluids is the possible occurrence of a peak in adsorption with pressure (Aranovich and Donohue, 1995, 1996). Its occurrence will depend on the gas type, the proximity of pressure and temperature conditions to the supercritical ('sc') state of the gas, the void volume determination technique, and the sample properties (e.g. pore size distribution) (Murata et al., 2001; Gumma and Talu, 2003; Herrera et al., 2011; Gasparik et al., 2012). Laboratory experiments thus should be performed at relevant subsurface pressure and temperature conditions, but often the experimental literature is restricted to lower pressures due to available equipment and experimental constraints.

In that context, CH<sub>4</sub>-CO<sub>2</sub>-shale adsorption processes are conveniently divided into three stages owing to the pressure range and adsorption rate: low pressure (<3 MPa; below supercritical conditions), intermediate pressure (3–10 MPa; transition into supercritical conditions) and high-pressure (>10 MPa; supercritical state) adsorption stages that vary depending on the gas species and sample properties. The low-pressure stage is characterized by sorption on the sites with highest adsorption energy (i.e. the smallest pores) first, and progression towards larger pores (as pressure increases) which causes gradual reduction in the isosteric heat of adsorption (Stoekli, 1990). This is indicative of physisorption by pore-filling as originally suggested by Dubinin (1975) for gas sorption in microporous materials. Further increase in pressure will eventually cause only small changes in the adsorption content. The isosteric heat of adsorption reduces with pressure until equilibrium is established, and no more gas can adsorb.

In the reviewed literature, CH<sub>4</sub> excess adsorption on gas shales is reported to increase monotonously with pressure (in both gaseous and supercritical states) and gradually reach a constant value at high pressures (Bi et al., 2016; Wang et al., 2016; Li et al., 2017). Gas-phase CO<sub>2</sub> adsorption also increases monotonously with pressure to the supercritical transition point, however adsorption of CO<sub>2</sub> in supercritical state causes the adsorption profile to reach a maximum, after which further increase in pressure will cause CO<sub>2</sub> to desorb monotonically. Typical



sorption behavior for both CH<sub>4</sub> and CO<sub>2</sub> is depicted in Fig. 2 for sorption experiments on crushed Devonian shale samples at a fixed temperature of 45 °C and pressures ranging up to 25 MPa. The characteristic difference in the adsorption of either gas is clearly revealed, with maxima observed only for CO<sub>2</sub>. The same trend in experimental profiles of CO<sub>2</sub>-CH<sub>4</sub> sorption is reported by Strubinger et al. (1991); Sudibandriyo et al. (2003); Busch et al. (2008); Weniger et al. (2010); Schaefer et al. (2013); Gasparik et al. (2014); Schaefer et al. (2014); Lu et al. (2016); Meray and Sinayuc (2016) on either gas shale samples of original composition or pure inorganic minerals.

In shales, the gradual increase in CO<sub>2</sub> adsorption near supercritical conditions has been attributed to the sharp change (i.e. increase) in fluid density when gaseous CO<sub>2</sub> is converted to supercritical fluid. This favors overall CO<sub>2</sub>-shale interaction by increased (binding) energy and more molecular layers are attached onto the surfaces. For CO<sub>2</sub>, Schaefer et al. (2013) observed that with continued adsorption, the cross-over point (Fig. 2b) is reached because the stabilization energy ( $E_{\text{inter-ad}}$ ) of the supercritical CO<sub>2</sub> molecules increases as the pressurized system brings the gas molecules closely together. Meanwhile, the adsorbate-adsorbent adsorption energy ( $E_{\text{ads}}$ ) decreases (becomes less negative). This could drive the adsorbent-adsorbent binding energy ( $E_b$ ) to negative ranges (see equation (3)) and thereafter desorption dominates as the principal mechanism and a decline is observed in the isotherm curve. Recently, Jia et al. (2018) reported a similar trend of CO<sub>2</sub> adsorption behavior, where a crossover region was observed before and after the critical pressure point, through sorption measurements from low-to high-pressure conditions (temperature was kept constant at 30 °C) in a shale core from the Green River Formation in Colorado. The discontinuity of CO<sub>2</sub> adsorption at pressures above CO<sub>2</sub>-P<sub>cr</sub> may have crucial implications on CO<sub>2</sub>-ESGR and CO<sub>2</sub> storage. It must be noted that the occurrence of an adsorption peak has also been reported in some cases for CH<sub>4</sub>, although mostly for dried overmatured gas shales (Moffat and Weale, 1955; Gasparik et al., 2012; Merkel et al., 2015; Zhou et al., 2018) and pure carbon adsorbents (Xiong et al., 2017). Most single- and multi-component adsorption isotherms are monotonous; showing no distinct peaks even at relatively high pressures (e.g. the Langmuir type). Capturing physical behavior at reservoir conditions may require more general isotherm approaches, especially when significant peaks and declines are demonstrated in lab measurements.

#### 4. Dependence of gas sorption on shale properties

Most sorption studies are available on gas shale samples of original composition or pure individual shale components. The literature indicates that shale adsorption capacity correlates directly to factors that

can generate more micropores, but inversely to factors that reduce or plug micropores. This is because small pores generate larger surface area and stronger adsorbate-adsorbent interaction energy which results in greater adsorption. Sorption experiments on samples from across the world (see Fig. 3) have been reviewed in this section to gain insight into the relationship between sorption, rock compositional and geological features to outline the major factors that controls gas sorption capacity of shales.

##### 4.1. Influence of organic matter (richness) on gas sorption

The shale organic matter (OM), also known as kerogen, is associated with the in-situ generation of hydrocarbons. The organic richness is frequently expressed by the Total Organic Carbon (TOC). It is primarily responsible for the microporous nature of shale and is the main contributor to the surface area and total pore volume (Cao et al., 2015; Zhou et al., 2018). The TOC wt% of the shale varies substantially among shale reservoirs and within a formation itself. Table 1 shows the TOC content reported for some shale gas plays. Although these values may not exactly be large, the microporosity associated with the organic fraction is the principal control on CH<sub>4</sub> and CO<sub>2</sub> sorption; there the trapping forces are enhanced due to coalescing of molecules and overlap of interaction energies between the sorbed gas molecules (Thommes, 2010). In stark contrast, immature gas shales with appreciable matrix bituminite can store gas by dissolution and may demonstrate large sorbed gas capacities that are unrelated to micropore volume (Ross and Bustin, 2009). Bituminite, originally described by Teichmüller (1971), could be considered as a semi-solid portion of degrading organic matter that lacks definite shape or form (Kus et al., 2017). It is often present in immature source rocks and may have a dominantly fluidal or granular internal structure within which gases could be stored by dissolution.

The reviewed literature confirms that CH<sub>4</sub> and CO<sub>2</sub> sorption capacities on shale is strongly correlated with TOC. A strong positive linearity is observed for CH<sub>4</sub> and CO<sub>2</sub> sorption datasets (Ross and Bustin, 2007a, 2008; 2009; Zhang et al., 2012; Wang et al., 2013; Heller and Zoback, 2014; Hong et al., 2016; Cancino et al., 2017; Zhou et al., 2018) sourced from experimental measurements on a wide range of shale samples (Fig. 4). The regression factors for both CH<sub>4</sub> and CO<sub>2</sub> are relatively high under both dry and moist conditions and demonstrate the shale TOC to have primary control on adsorption of either gas species. It is interesting to note that the regression constants for both species is higher for moisture-equilibrated samples relative to dry samples. This implies a much stronger correlation of gas adsorption to TOC in the presence of water and could infer that water adsorbs primarily to water-wet inorganic (i.e. clay) mineral phases within the shale formation.

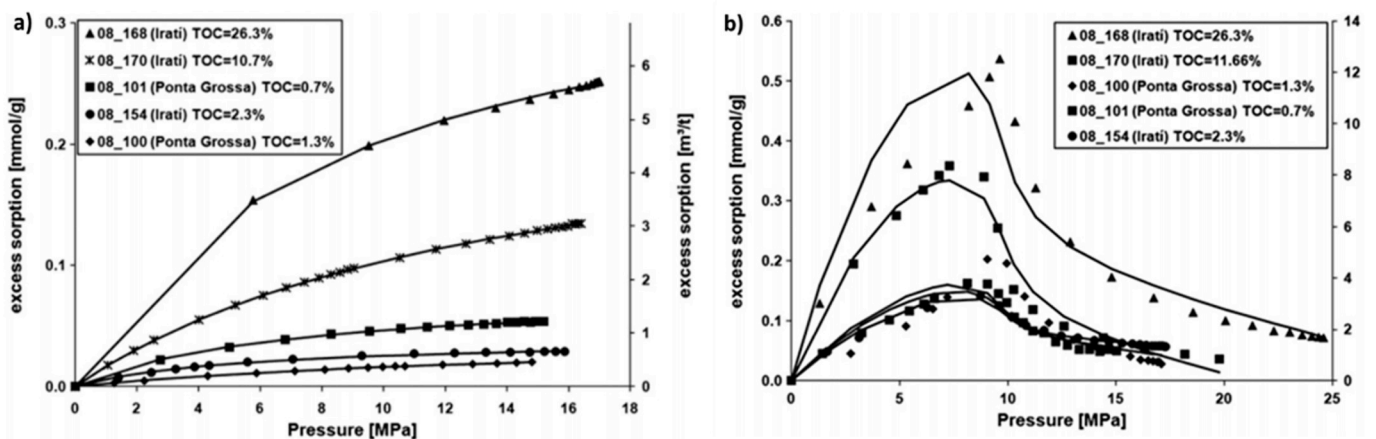
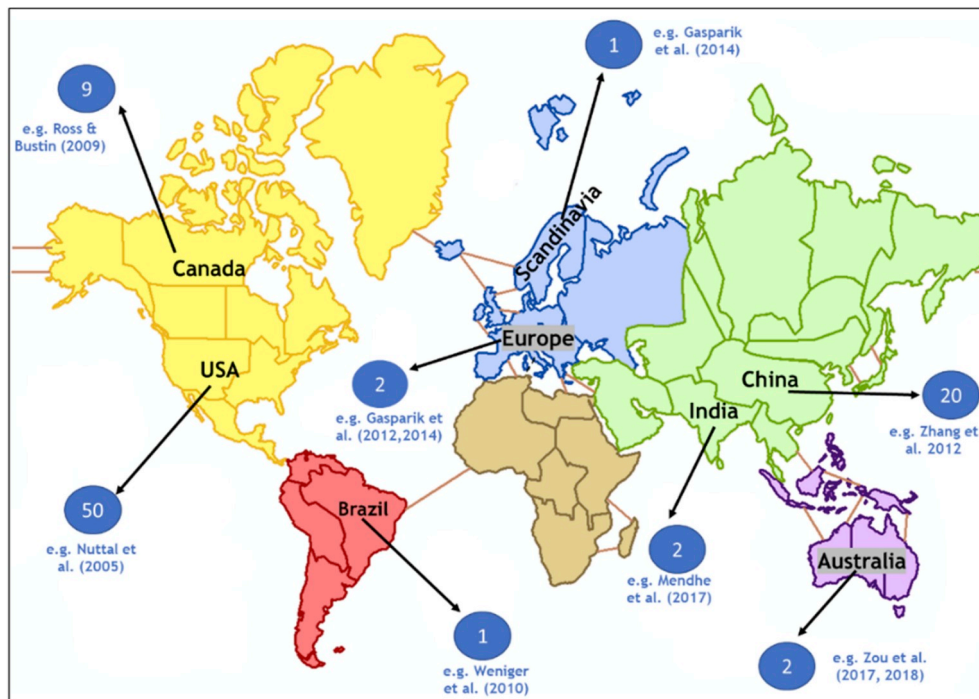


Fig. 2. Comparison of adsorption isotherm (excess sorption vs pressure) for CH<sub>4</sub> (a) and CO<sub>2</sub> (b) on gas shale samples of the Paraná Basin in Brazil (Weniger et al., 2010). Experiment was conducted on crushed dry samples at a fixed temperature of 45 °C.



**Fig. 3.** Worldwide illustration of shale formations actively investigated by researchers. The numbers are purely based on the literature reviewed in this study with focus particularly on CH<sub>4</sub> and CO<sub>2</sub>, sorption tests and auxiliary evaluations relevant to CO<sub>2</sub>-ESGR.

**Table 1**

Typical TOC of some shale plays and formations (fm.) adapted from Chalmers and Bustin (2007); Ross and Bustin (2007a, 2008); Ambrose et al. (2010); Zhang et al. (2012); Wang et al. (2013).

| Region                                       | Shale/Play               | TOC (wt %) |
|--|--------------------------|------------|
| North – American Shale systems, U.S          | Barnett                  | 2.5–7.9    |
|  | Marcellus                | 1–10       |
|  | Haynesville              | 0–8        |
|  | Horn River               | 3          |
|  | Woodford                 | 5          |
| Northeastern British Columbia region, Canada | Lower Jurassic fm.       | 0.8–11.8   |
|  | Lower cretaceous fm.     | 0.53–17    |
| Western Canada Basin                         | Poker Chip fm.           | 0.8–2.2    |
|  | Besa River fm.           | 0.9–5.7    |
|  | Horn River fm.           | 2.5–3.5    |
|  | Muskwa fm.               | 0.4–3.6    |
|  | Fort Simpson fm.         | <1         |
| Sichuan Basin, China                         | Mattson                  | <1.2       |
|  | Qiong-zhu-si fm.         | 0.5–4      |
|  | Long-ma-xi fm.           | 0.5–2.3    |
|  | Da-long and Long-tan fm. | 1.0–10     |

It is noted that extrapolating the regression lines to TOC concentrations of zero reveals the influence of other non-organic adsorption sites, hence significant deviations from this trend could be observed for individual samples depending on the compositional makeup. High-pressure gas sorption isotherms reported by Tan et al. (2014) showed sorption capacities of samples with similar clay content, thermal maturity and moisture content to exhibit even stronger positive linear correlations with TOC. The dependence of gas adsorption on TOC content has been reported by many other researchers (Manger et al., 1991; Schettler and Parmely, 1991; Lancaster and Hill, 1993; Lu et al., 1995; Zuber et al., 2002; Chalmers & Bustin, 2007, 2008; Ross and Bustin, 2007a; Ruppel and Loucks, 2008; Beaton et al., 2010; Strapoc et al., 2010; Weniger et al., 2010; Chareonsuppanimit et al., 2012; Wei et al., 2012; Gasparik et al., 2014; Rexer et al., 2014; Bi et al., 2016; Wang

et al., 2016; Yang et al., 2016; Chang et al., 2017; Mendhe et al., 2017; Xia et al., 2017; Sharma and Galvis-Portilla, 2018). There are however existing studies that have reported little to no correlation between TOC and adsorption capacity (Gasparik et al., 2012; Zou et al., 2017). This trend is particularly notable in shales with low organic matter content and high clay content.

#### 4.2. Influence of thermal maturity

Thermal maturity describes the heat-driven diagenetic changes of organic matter in sedimentary source rocks to generate hydrocarbons. Vitrinite reflectance,  $V_r$ , is widely used as indication of thermal maturity in shale analysis. It is measured by optical microscopy and reported by %  $R_o$  (where high % $R_o$  indicates high maturity), the percentage of incident light reflected from the surface of vitrinite particles in the shale rock. In shales, thermal maturity of organic matter can generate additional micropores (Bae and Bhatia, 2006; Jarvie et al., 2007; Chalmers and Bustin, 2008; Loucks et al., 2009; Ambrose et al., 2010; Sondergeld et al., 2010; Curtis et al., 2011; Bernard et al., 2012; Ma et al., 2015; Wu et al., 2017; Delle Piane et al., 2018; Zheng et al., 2018). This is due to the structural transformation of organic matter during maturation that generates smaller (nano-micro scale) pores as kerogen is thermally converted. The generation of more micropores with organic matter maturity increases the adsorption capacity.

It was previously suggested (Ramos, 2004) that the strong correlation between sorption and TOC masks the relationship between adsorption capacity and thermal maturation. However, Ross and Bustin (2009) found the sorption capacities of low TOC (0.2–4.9 wt%) over-mature D-M shale samples ( $1.6\% < R_o < 2.5\%$ ) to be higher than for high TOC (1.4–11.8) immature Jurassic shales ( $R_o < 1.2\%$ ). This was qualitatively attributed to creation of sorption sites, and/or opening up microporosity onto which gas could sorb from structural transformations of the organic matter during thermal maturation. Nonetheless, other researchers have found concomitant decrease in CH<sub>4</sub> sorption capacity with increasing maturity (Chalmers and Bustin, 2007, 2008). This suggests, as previously pointed out by Schieber (2010) that

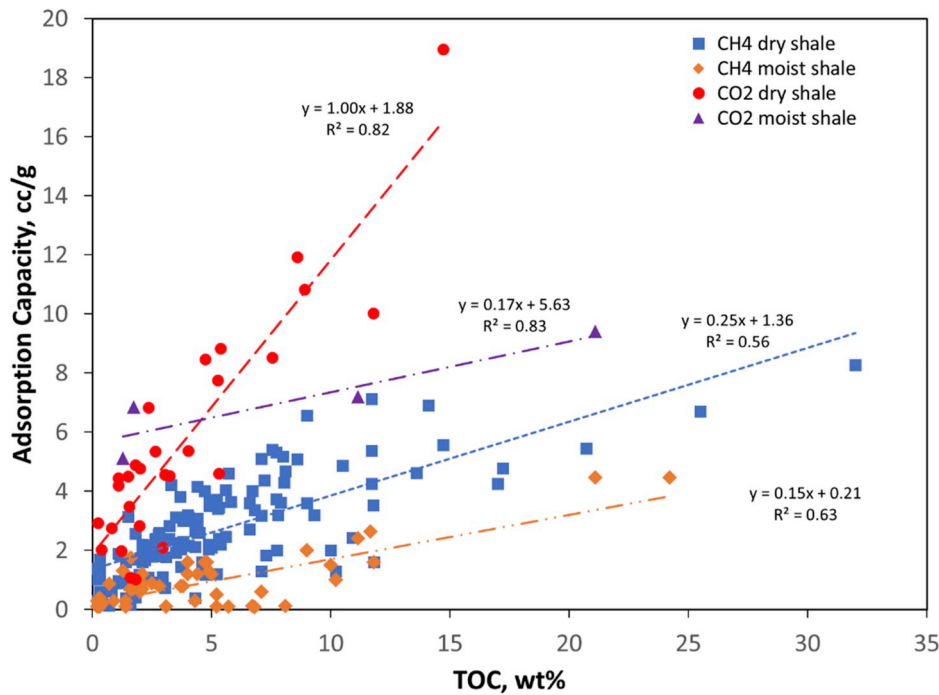


**Fig. 4.** Correlation between TOC and CH<sub>4</sub>, CO<sub>2</sub> sorption capacity of dry and moisture equilibrated shales. Data points are representative of langmuir volume reported in the evaluations of (Nuttal et al., 2005; Ross and Bustin, 2009; Weniger et al., 2010; Zhang et al., 2012; Wang et al., 2013; Gasparik et al., 2014; Heller and Zoback, 2014; Luo et al., 2015; Hong et al., 2016; Cancino et al., 2017; Pozo et al., 2017; Zhou et al., 2018). The regression constants of both species are relatively high and extrapolation to zero TOC content shows impact of auxiliary sorption sites.

intraparticle OM pore generation in thermally matured rocks may depend on the OM type. Loucks et al. (2012) also reported absence of OM pores in a matured ( $R_o$  of 0.89%) shale sample from the Atoka formation in the Midland Basin. The relationships established for any specific shale system, therefore, may not be directly applied elsewhere. But in general, the reviewed literature indicates that overmature and high TOC samples will show higher sorption capacity for both CH<sub>4</sub> and CO<sub>2</sub> than the low mature and low TOC shales.

Some literature also reports thermal maturity to have noticeable effect on the shape of excess isotherms. Zhang et al. (2012) reported the methane Langmuir pressure,  $P_L$  of three Barnett shale samples (%  $R_o = 0.58, 0.81, 2.01$ ) to distinctly shift towards lower pressures from the immature to overmature gas shale samples under the same temperature conditions. Similar trends have been reported by Gasparik et al. (2014) and Tan et al. (2014). In a related study, Gasparik et al. (2012) also found positive correlation between TOC-normalized sorption capacities and maturity for black shales, but the trend became negative for over matured samples with  $R_o$  in a range of 2.8–3.3%.

#### 4.3. Influence of kerogen type

Although TOC content has a superior control on gas sorption in shales, another key factor is kerogen type. Kerogen is the fraction of organic matter in sedimentary rocks (in this case, shale rocks) that is insoluble in organic solvents. It is formed from the decomposition of organic matter and is the precursor of hydrocarbon generation in source rocks. Kerogen is categorized as either Type I, which consists mainly of algal and amorphous kerogen and is highly likely to generate oil; Type II, which is formed from mixed terrestrial and marine source materials and can generate both oil and gas (but mostly waxy oil); and Type III, which is formed from terrestrial plant debris and typically generates gas upon maturation. In essence, the kerogen type depends on the source rock material and the deposition environment (Seewald, 2003; Boyer et al., 2006; Vandenbroucke and Largeau, 2007; Glorioso and Rattia, 2012).

Chalmers and Bustin (2008) investigated CH<sub>4</sub> sorption capacity for the Lower Cretaceous Buckingham Formation in Canada and found that per unit TOC volume basis, the capacity trend was Type II/III mixtures > Type III > Type II > Type I. They attributed this to Type III

kerogen being more mature and generating more hydrocarbons and micropores at a given temperature compared to the other kerogen types. Zhang et al. (2012) conducted high pressure (0–16 MPa) methane sorption tests on organic-rich bulk shale samples and their isolated kerogens, with thermal maturity and kerogen type being the main variation in the samples. At all temperature conditions (35, 50, 65 °C), the CH<sub>4</sub> sorption capacity was in the order of Type III > Type II > Type I (Fig. 5). The trend was attributed to extensive aromatization from immature (Type I) to overmature (Type III) organic matter. They indicated that the progression from kerogen Type I to Type III, represents an increase in the relative fraction of aromatic hydrocarbons compared to the aliphatic and naphthenic hydrocarbons, as reported by other researchers (Tissot and Welte, 1984; Helgeson et al., 2009). The findings of Zhang et al. (2012) depict methane adsorption to be influenced by the chemical structure of the organic matter. The details and concept of the effects exerted by organic functional groups on gas adsorption, particularly CO<sub>2</sub> is not well addressed in the literature and deserves further investigation. We also note, as indicated by Loucks et al. (2012) that different kerogen types exhibit differing propensities to the development of intraparticle OM pores. The storage capacity trend reported for a shale Basin system based on kerogen types may therefore not be applicable to shales from different Basins. This complicates the generalization of the effects that kerogen type exerts on adsorption capacity. We recommend further studies on the association of OM pores and kerogen type to elucidate this phenomenon.

#### 4.4. Influence of inorganic components

Shale usually contains clay, quartz or carbonate mineral phases with trace amounts of albite and pyrite. These inorganic constituents contribute enormously to the surface area and influence pore size, cumulative porosity and sorption properties. Particularly, the clay minerals are reported (Slatt and O'Brien, 2011; Milliken et al., 2013) to contribute to the shale micropore volume. In contrast to coals, where mineral matter seems to have little influence on CH<sub>4</sub> sorption capacity (e.g. Faiz et al., 1992; Rice et al., 1993; Bustin and Clarkson, 1998) but significantly affects CO<sub>2</sub> sorption (e.g. Karacan and Mitchell, 2003; Weniger et al., 2010), mineral components in gas shale systems have



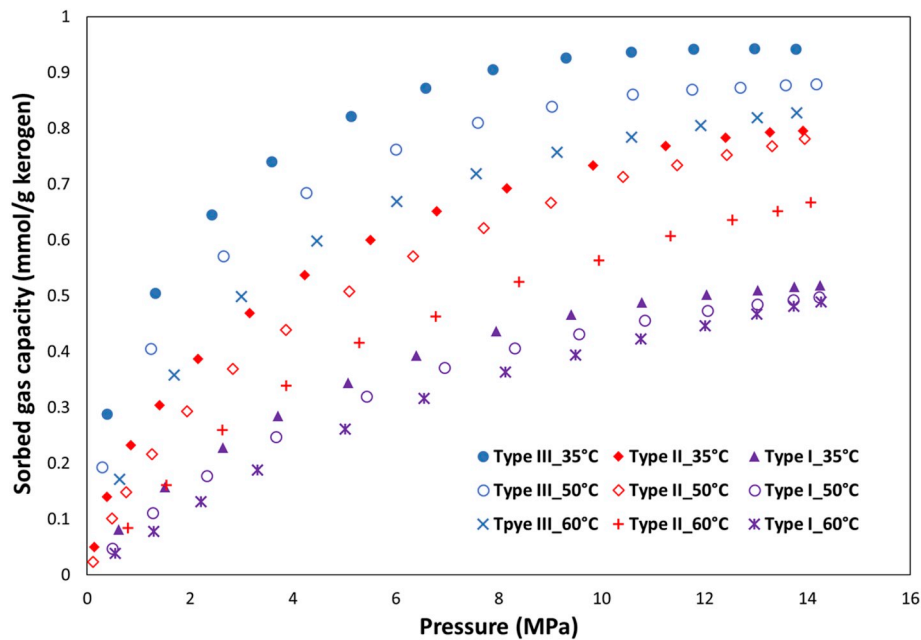


Fig. 5. Effect of kerogen type on methane sorption capacity at different temperatures (Zhang et al., 2012).

been proven to have appreciable sorption capacity for both gases (Aylmore, 1974; Heller and Zoback, 2014).

Preliminary adsorption studies on Devonian gas shale samples by Schettler and Parmely (1991); Lu et al. (1995) exclusively highlighted the inorganic clay minerals to contribute as sorption sites in shale systems due to their microporous nature. Schettler and Parmely (1990) originally postulated TOC to be of secondary importance in shale systems with low organic content. This conclusion was later reiterated by Busch et al. (2008) who attributed the high CO<sub>2</sub> sorption capacity of Muderong shales (TOC < 0.5%) entirely to its clay mineral constituents. The strong positive correlation of shale clay content to sorption capacity is emphasized in other reports (Chalmers and Bustin, 2008; Gasparik et al., 2012; Luo et al., 2015; Wang and Yu, 2016; Lutyński et al., 2017) where low TOC shale samples demonstrated high sorption due to their high clay contents. The specific influence of clay on shale sorption, however, is less evident in shales with high TOC content (Wang et al., 2013; Gasparik et al., 2014; Tan et al., 2014; Bi et al., 2016).

The microporous crystal layers of clay serve as ideal adsorption sites due to the large surface area (Aringhieri, 2004; Cheng and Huang, 2004; Venaruzzo et al., 2002). The contributions differ with clay type. Ross and Bustin (2009) reported clay-rich (low Si/Al ratio) shales to have superior gas storage capacities over their silica-rich (high Si/Al ratio) counterparts. Ji et al. (2012) conducted sorption experiments (up to 15 MPa) on dried clay-rich rocks at varying temperatures (35–65 °C) to shed light on the relative influence of clay type on methane adsorption. They established physisorption as the dominant mechanism for CH<sub>4</sub> adsorption on clay and noted sorption capacity to proceed in the order of montmorillonite > illite/smectite mixed layers > kaolinite > chlorite > illite. High-pressure CO<sub>2</sub> sorption experiments on pure clay minerals showed Ca-rich montmorillonite to have greater storage capacity than Na-rich montmorillonite (Busch et al., 2008). Gas shale reservoirs are dominated by illite (Jarvie et al., 2001; Gasparik et al., 2012), possibly due to the illitization of kaolinite and smectite which occurs at temperatures between 80 and 120 °C (Pytte and Reynolds, 1989). The temperatures of high organic content shale systems is in the range 96–277 °C (Lu et al., 2016). It is likely that at adequate conditions (especially in tropical zones) a blend of chemical and temperature gradient change could trigger a transition from illite to smectite (Eberl, 1984). This may occur particularly for uplifted shales exposed to weathering (e.g. shallow reservoir sections and outcrops). Since smectite

has larger surface area (Šucha et al., 2001) and thus greater sorption, this could lead to potential overestimation of gas storage capacity during shale gas exploration. Additional study is recommended to understand the possibility of illite-smectite reversal transformation in clays found in shale formations.

It must be pointed out that clays are naturally hydrophilic and may present experimental challenges when correlating shale sorption capacity to clay content. For example, Chalmers and Bustin (2008) observed that the TOC-normalized CH<sub>4</sub> sorption capacity in dry samples from the Bucking horse formation in Canada positively correlated with clay content whereas no correlation existed for moisture equilibrated samples. Data obtained from as received or moisture equilibrated, and dried samples should therefore be evaluated carefully to accommodate this fundamental clay-water affiliation.

#### 4.5. Influence of moisture

Moisture is reported to correlate positively with organic matter and clay content in shale formations (Chalmers and Bustin, 2007; Passey et al., 2010) which makes it a crucial subsurface component to be analyzed in sorption experimental procedures. Many authors have addressed the effect of moisture on gas adsorption by comparing the adsorption capacity of dry samples and moisture equilibrated samples (Lu et al., 1995; Ross & Bustin, 2007a, 2009; Busch et al., 2008; Gasparik et al., 2012, 2014; Aljamaan, 2013; Tan et al., 2014; Yuan et al., 2014; Yang et al., 2016; Zou et al., 2018) The result indicates that sorption capacity decreases with increasing moisture content until a certain equilibrium (critical) moisture content is attained for the sample. This equilibrium moisture content is representative of the maximum moisture saturation that can adsorb on the shale surfaces.

When present, water sorbs strongly on organic functional groups containing oxygen via hydrogen bonding (Dubinin, 1980) and has secondary tendencies to interact with pre-adsorbed water and charged surfaces of mineral matter (especially chemisorptive clay). Thus, besides attaching to primary (water-wet) sorption sites in the clay matrix, molecular water also competes with CO<sub>2</sub> and CH<sub>4</sub> for adsorption sites and causes a reduction in the gas sorption capacity. In shales, besides attaching onto surfaces, water molecules can condense in inorganic pores, occupying the smaller capillaries first before filling the larger pores as relative humidity increases (Zolfaghari et al., 2017a, 2017b).

The water molecules can also aggregate as clusters at high pressure (Aljamaan, 2013; Yang et al., 2016; Huang et al., 2018) to block gas-enterable pores and serves as an added negative effect on gas sorption capacity.

The equilibrium moisture content depends on the shale maturity, organic richness and organic type (Chalmers and Bustin, 2008). The value for selected European gas shale samples was estimated (Gasparik et al., 2014) to be at or below 75% relative humidity (RH). Merkel et al. (2015) reported similar values for the moisture saturation threshold (50–75% RH) of Bossier and Haynesville shales from the U.S. A recent report by Fan et al. (2018) indicated that the methane sorption capacity versus moisture content exhibited three distinct decreasing stages separated by two threshold moisture contents (Fig. 6). They performed CH<sub>4</sub> sorption experiments on gas shale samples from the Sichuan Basin in China at 35, 45 and 55 °C and pressures up to 10 MPa. They attributed the initial reduction (stage I) to competitive adsorption between water and methane until an extended stagnant period (stage II) where all possible hydrophilic sites are filled. They postulated that water condensation in the clay pores and some organic hydrophobic pores was responsible for the late convex-like decrease (stage III) in the adsorption capacity. The moisture effect is however reported to be masked in high TOC and over mature gas shales (Ross and Bustin, 2007a; Wang and Yu, 2016).

#### 4.6. Influence of temperature

Thermodynamically, adsorption is an exothermic process and the effect of changing the equilibrium temperature is hinged to the Le Châtelier principle. Therefore, less adsorption is expected with increasing temperature. This relation was first reported for shales by Lu et al. (1995) who investigated sorption as a function of both pressure and temperature on Devonian shales and showed the sorption capacity to decrease with temperature. Recently, Mery and Sinayuc (2018) confirmed through adsorption measurements at 25, 50 and 75 °C that adsorption capacity increases for both CH<sub>4</sub> and CO<sub>2</sub> when temperature is decreased. This concurs with other experimental evaluations (Guo, 2013; Guo et al., 2013; Hao et al., 2013; Fan et al., 2014; Duan et al., 2016; Chang et al., 2017; Pozo et al., 2017; Zou et al., 2017; Liu et al., 2018).

Zhang et al. (2012) reported that the decrease in sorptive capacity with temperature occurred on both bulk gas shale samples (of original composition) and their isolated kerogens. Gasparik et al. (2014) constructed methane isotherms at experimental temperatures ranging up to 100 °C for immature ( $V_r = 0.5$ ) and mature ( $V_r = 0.9$ ) shale samples and up to 150 °C for over-mature ( $V_r = 1.5$ ) samples and reported that besides reduction in sorptive capacity, this sorption capacity was reached at a higher pressure when the temperature was increased. This implies that for the same sample, adsorption capacity decreases with

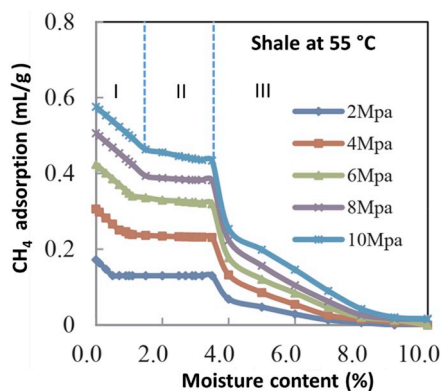


Fig. 6. Effects of moisture content on methane maximum sorption capacity at 55 °C (Fan et al., 2018).

temperature and that less gas can adsorb at lower pressures. The interrelation of adsorbed gas amount with temperature and pressure is depicted in Fig. 7.

#### 5. CO<sub>2</sub> versus CH<sub>4</sub> sorption on shale

The first investigation of CO<sub>2</sub> and CH<sub>4</sub> sorption on the same shale material was conducted by Nuttal et al. (2005). They measured isothermal CH<sub>4</sub> and CO<sub>2</sub> adsorption on several Devonian black shales from Kentucky and found CO<sub>2</sub> absolute mass adsorption to be approximately 5 times greater than that of CH<sub>4</sub> at the same pressure. Following their report, several authors (Weniger et al., 2010; Kang et al., 2011; Chareonsuppanimit et al., 2012; Aljamaan, 2013; Heller and Zoback, 2014; Luo et al., 2015; Charoensuppanimit et al., 2016; Hong et al., 2016; Cancino et al., 2017; Pozo et al., 2017) have performed CO<sub>2</sub> and CH<sub>4</sub> gas sorption measurements on the same gas shale sample under controlled experimental conditions and reported consistently higher CO<sub>2</sub> sorption relative to CH<sub>4</sub>. The reported CO<sub>2</sub>/CH<sub>4</sub> absolute mass sorption ratio ranges between 1.3 and 10 for dry shale samples (Fig. 8). The ratio is expected to be relatively lower at moist conditions for the same shale sample since sorption capacity in general is lower for moist shales (see Fig. 4). There is limited data in the literature that compares the CO<sub>2</sub>/CH<sub>4</sub> sorption ratio for the same sample at dry and moist conditions. Such an experimental study would be relevant to confirm this trend.

The relative sorption capacity of gas shale materials for either CO<sub>2</sub> or CH<sub>4</sub> is controlled by the respective interaction energy (thermodynamic forces), molecular size and accessibility of each gas type to the microporous network of the shale matrix system (steric forces). The tetrahedral molecular geometry of CH<sub>4</sub> is somewhat rounded, compared to CO<sub>2</sub> which has a linear molecular geometry. The dynamic diameter of CO<sub>2</sub> is about 0.33 nm as compared to 0.38 for CH<sub>4</sub> (Duan et al., 2016). The effective size of CO<sub>2</sub> is therefore smaller and can access narrower pores in the shale matrix and contacts a greater volume of the shale system (Kang et al., 2011). The reviewed experimental results depict that the steric and thermodynamic controlling parameters favor adsorption of CO<sub>2</sub> over CH<sub>4</sub> in gas shales. The mechanism of CO<sub>2</sub> accessibility is reportedly enhanced at supercritical conditions where gaseous CO<sub>2</sub> transitions to supercritical CO<sub>2</sub> (Sc-CO<sub>2</sub>). Sc-CO<sub>2</sub> is completely wetting to the shale rock, with liquid-like density, but with viscosity and diffusive properties close to gas behavior (Wang et al., 2012). This unique physicochemical feature can improve the volumetric sweep during CO<sub>2</sub> injection and potentially increase the CO<sub>2</sub> subsurface storage amount by allowing Sc-CO<sub>2</sub> to contact more available sorption sites deeper within the formation.

Binary CO<sub>2</sub>-CH<sub>4</sub> and mixed-gas sorption experiments evaluating the selectivity of gas shales for either gas species under the same pressure and temperature conditions have also been recently reported on the same shale sample in the literature. In these tests, a gas detection device (e.g. gas chromatograph) supplements the conventional sorption experimental setup that allows the determination of the gas mole fraction of each species in the mixture. During the tests, the shale samples are initially saturated with varied molar ratios of CO<sub>2</sub> and CH<sub>4</sub> at the desired experimental conditions. The majority of these authors (Pusch et al., 2012; Luo et al., 2015; Duan et al., 2016; Cancino et al., 2017; Huang et al., 2018; Ma et al., 2018) observed preferential adsorption of CO<sub>2</sub> over CH<sub>4</sub>. It is reported that the selectivity of CO<sub>2</sub> in a gas mixture experiment evolves with pressure and is significantly higher at low pressures (Cancino et al., 2017) most likely due to the dominance of micropore filling associated with low temperatures. The adsorption selectivity parameter (represented as  $\alpha$ ) is frequently used to evaluate the competitive adsorption between CO<sub>2</sub> and CH<sub>4</sub> and given as (Duan et al., 2016):

$$\alpha_{CO_2/CH_4} = \frac{x_{CO_2} y_{CH_4}}{x_{CH_4} y_{CO_2}} = \frac{V_{LCO_2} / P_{LCO_2}}{V_{LCH_4} / P_{LCH_4}} \quad (4)$$



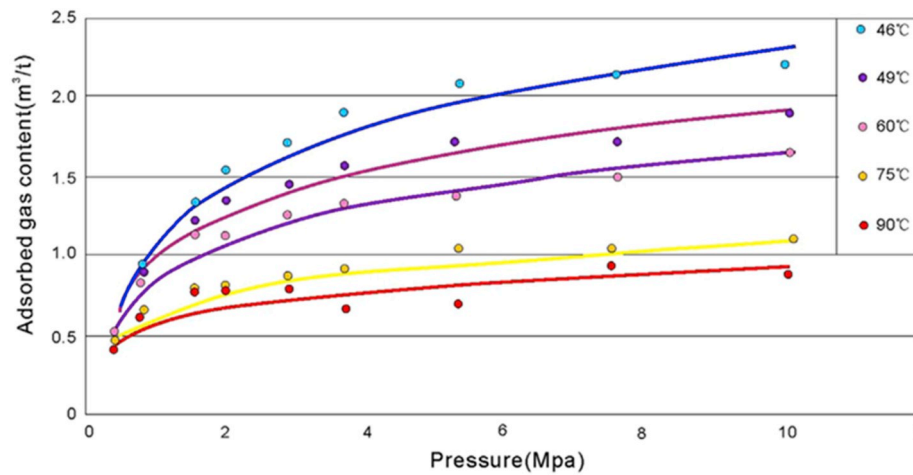


Fig. 7. Variation of adsorbed CH<sub>4</sub> amount with temperature performed on gas shale samples of the Ordos Basin in China (Guo, 2013).

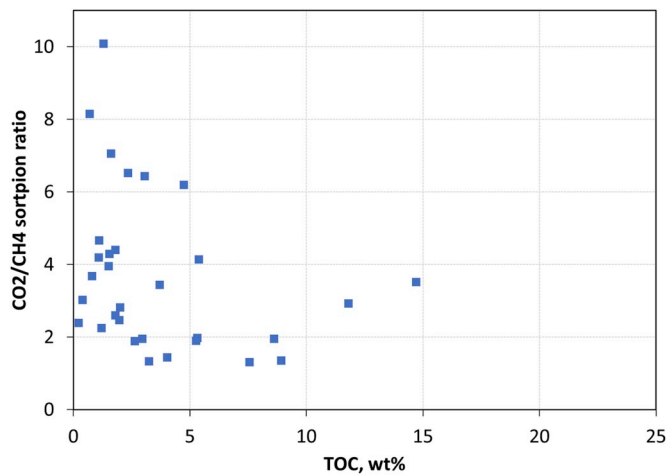


Fig. 8. CO<sub>2</sub>/CH<sub>4</sub> sorption ratio for different dry shale samples as a function of total organic carbon content. Data sets are taken from Langmuir volumes reported in the evaluations of Nuttal et al. (2005); Heller and Zoback (2014); Luo et al. (2015); Hong et al. (2016); Cancino et al. (2017); Pozo et al. (2017).

where  $x$  and  $y$  variables are the molar fractions of the gas species in the adsorbed phase and free gas phase respectively for gas mixture evaluations and  $V_L$ ,  $P_L$  are the Langmuir parameters. A value of  $\alpha_{CO_2/CH_4} > 1$  suggests that adsorbed CH<sub>4</sub> can be displaced by CO<sub>2</sub>. Larger values represent stronger displacement capacity of CO<sub>2</sub> over CH<sub>4</sub>. The CO<sub>2</sub> selectivity over CH<sub>4</sub> depends on shale matrix composition and pore structure. For iso-TOC samples, high clay content and micropores favours higher  $\alpha_{CO_2/CH_4}$  (Duan et al., 2016). The variation of  $\alpha_{CO_2/CH_4}$  for some selected shales in China and the U.S are shown in Fig. 9 where the selectivity is seen to decrease with increasing TOC.

In coals, preferential adsorption of CH<sub>4</sub> over CO<sub>2</sub> in mixed-gas sorption experiments has been reported, particularly at low pressures (Crosdale, 1999; Busch et al., 2003, 2006; Majewska et al., 2009). In shale samples, however, consistent CO<sub>2</sub> preferential adsorption in the entire pressure range has been experimentally proven and verified by simulation studies (e.g Mery and Sinayuc, 2016). These experiments are however limited, and further studies of multi-component sorption in gas shales is recommended to validate the trend.

## 6. Current practice of dynamic CO<sub>2</sub>-CH<sub>4</sub> exchange

In gas shales, the experimental approaches to evaluate CO<sub>2</sub>-CH<sub>4</sub>

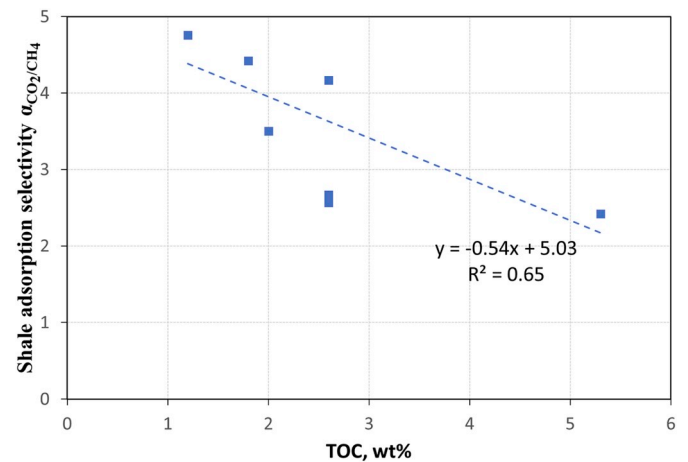


Fig. 9. Variation of shale adsorption selectivity  $\alpha_{CO_2/CH_4}$  different dry shale samples from China and the U.S as a function of total organic carbon content (Heller and Zoback, 2014; Pei et al., 2015; Duan et al., 2016; Cancino et al., 2017).

exchange and gas recovery have been conducted implicitly by measuring how effectively CO<sub>2</sub> can replace already adsorbed CH<sub>4</sub> in a closed system. The procedures differentiate between the CO<sub>2</sub> and CH<sub>4</sub> molecules existing as adsorbed or free phase throughout the dynamic CO<sub>2</sub>-CH<sub>4</sub> exchange within the shale sample at specific time steps. During these tests, usually shale material (which is often crushed) is initially saturated with CH<sub>4</sub> at desired experimental conditions and allowed to equilibrate before CO<sub>2</sub> is injected at specified criteria. The CH<sub>4</sub> recovery yield is quantified by the resulting amount of originally adsorbed CH<sub>4</sub> released from the adsorbed state.

Some authors have employed the usual Gibbsian surface excess (GSE) variable for computations through the application of conventional sorption techniques (see Section 3), whereas others have used fluid detection techniques, like Nuclear Magnetic Resonance (NMR), for evaluation. NMR characterizes the existing states of hydrogen (<sup>1</sup>H) proton-containing fluids existing within a porous media (Coates et al., 1999). NMR-based techniques have been used successfully for petrophysical characterization of nano-porous structures in coal and gas shale (Mullen, 2010; Jin et al., 2017; Yin et al., 2017b; Zhou et al., 2018), monitoring flow and dispersion in porous media (Manz et al., 1999), evaluating CO<sub>2</sub> and CH<sub>4</sub> self-diffusion (Pusch et al., 2012) and CO<sub>2</sub> sorption on rock surfaces (Bernin and Hedin, 2018). A summary of the various findings from CO<sub>2</sub>-CH<sub>4</sub> exchange tests are presented in Table 2.

## 7. Discussion and key research issues

A vast amount of investigations have been carried out to study the effectiveness and feasibility of CO<sub>2</sub>-ESGR. However, some key research issues should be looked into:

- The majority of experimental work reported in the literature is conducted on crushed samples. To our knowledge, only Nuttal et al. (2003) reported adsorption data acquisition using an intact core. Their report highlighted the experimental difficulty involved since they only managed to capture CO<sub>2</sub> adsorption isotherm data for a single whole core out of twenty-six Devonian black shale samples. Using crushed samples is a quick and convenient means to perform measurements on shales, but an obvious trade-off is uncertainty in whether the data would be representative of actual reservoir conditions since it alters the structure of the porous medium (e.g. micro-fractures) and could lead to misrepresentative estimates of formation characteristics.
- The impact on gas sorption (i.e. isotherm shape) from organic matter content (TOC) and maturity, temperature and pressure and clay and moisture content are all relations that deserve attention. Particularly, lowered P<sub>L</sub> values (associated with decreasing temperature or higher maturity) indicate that CH<sub>4</sub> will desorb more readily at lower pressures on higher maturity shales. Such affinity to remain sorbed in matured shales indicates that a greater reduction in CH<sub>4</sub> partial pressure will be required to desorb CH<sub>4</sub> during production. The selectivity of the surface towards CO<sub>2</sub> can be the solution to release the strongly sorbed CH<sub>4</sub> and is in such cases even more important to measure. The question of how significant adsorbed gas will be to overall production is a key concept and further investigation is required to properly correlate the P<sub>L</sub> reduction to these parameters. Furthermore, measuring the density of the adsorbed gas phases is a key parameter in the commonly used modelling approaches that has not received much attention in experimental assessments.
- A notable concern for CO<sub>2</sub>-ESGR is the impact of moisture which preferentially binds to hydrophilic clay surfaces and reduces sorption (and hence CO<sub>2</sub> sequestration) potential. Dried samples may overestimate the adsorption capacity. Although water in principle like CO<sub>2</sub> can substitute CH<sub>4</sub> by adsorbing to hydrophilic surfaces and give EGR, water will usually exist also in aqueous phase and cause mobility issues related to presence of multiple phases and water blocking effects near the wellbore or macro-fractures. Pressurized

fracking fluids are essential for creating flow paths in the reservoir. The standard is use of water, but there is potential in using water-free fracking methods (e.g. propane-gel, supercritical CO<sub>2</sub>). Gas soluble fracking fluids should be positive for recovery as well as the environment (reduction of produced water).

- Reports (Heller and Zoback, 2014; Lu et al., 2016; Yin et al., 2016) indicate crushed shale to swell (especially for high clay-content shales) during gas adsorption which changes both the pore structure and roughness. The degree of adsorption-induced swelling is shown to vary depending on the shale composition and pore characteristics and achieves a stable state when adsorption equilibrium is attained. The extent to which swelling during CO<sub>2</sub> injection impacts sorption isotherms, rock mechanical and hydrological (permeability, porosity) properties is crucial. In particular, Guo et al. (2017) observed through series of experiments that adsorption effects had substantial impact on shale permeability both at low and high pressures.
- Mechanical weakening of organic-rich gas shales by CO<sub>2</sub> saturation has been reported, especially for supercritical CO<sub>2</sub> (Lyu et al., 2016a, 2016b, 2018a, 2018b; Yin et al., 2017a) This is attributed to the modification of in-situ acid-base equilibria that triggers precipitation and dissolution of minerals (Liu et al., 2012; Carroll et al., 2013) and the ability of supercritical CO<sub>2</sub> to act as an organic solvent to extract non-polar aliphatic and polycyclic aromatic hydrocarbons from shale (Jiang et al., 2016; Yin et al., 2016). This could expand originally present gas seepage channels or generate flow channels with influence on the safety of sequestered CO<sub>2</sub>. Most of the experimental results are reported for gas saturated shale samples monitored over a couple of days.
- Geochemical alterations of Australian Muderong shales were suggested to explain differences in specific surface areas before and after CO<sub>2</sub> sorption experiments conducted at reservoir conditions (T = 45–50 °C; P < 20 MPa) (Busch et al., 2008). The inferred geochemical changes however could not be quantified and seemed to occur only at high pressures. In a subsequent study, Busch et al. (2009) assessed the interrelation of CO<sub>2</sub>-mediated reactions and transport properties in the Muderong shale by exposing crushed samples to CO<sub>2</sub> in the presence of water at 15 MPa and 50 °C for different equilibration time periods. They reported significant changes (equilibration times < 1 month) in mineralogical composition, particularly with the increase of smectite and K-feldspar contents and reduction in illite content. Mineral changes in shale sample

**Table 2**  
Experimental studies of CO<sub>2</sub>-CH<sub>4</sub> dynamic exchange conducted on shales.

| Author (s)           | Location               | Procedure  | Operating Conditions   | Findings   | Cons   |
|----------------------|------------------------|--|--|--|--|
| Huo et al. (2017)    | Longmaxi shales, China | Volumetric-based method applied to dried crushed samples               | Fixed temperature of 45 °C. Constant initial equilibrium pressure of CH <sub>4</sub> of 4.5 MPa CO <sub>2</sub> injection at varied pressures of 5.2, 6.3, 7.3, 8.4, and 9.3 MPa. Final system equilibrium pressures ranged were 4.7, 5.6, 6.5, 7.5 and 8.4 MPa respectively | The amounts of recovered CH <sub>4</sub> and stored CO <sub>2</sub> increase with CO <sub>2</sub> injection pressure. CH <sub>4</sub> recovery yield was higher for shales with smaller micropores (i.e. having lower CH <sub>4</sub> adsorption performance)  | Inherent uncertainties of evaluating excess sorption measurements. Final system equilibrium pressure not allowed to reach injection value. It is unclear what determined when to stop the test for each injection pressure step                        |
| Liu et al. (2017)    | Longmaxi shales, China | Nuclear Magnetic Resonance (NMR) based method on dried crushed samples | Fixed temperature of 35 °C. Varied initial equilibrium pressure of CH <sub>4</sub> -saturated sample of 0.1 MPa and 1.5 MPa CO <sub>2</sub> injected at constant pressure of 4.5 MPa   | CO <sub>2</sub> injection improved recovery yield of CH <sub>4</sub> in the adsorbed phase by an additional ~25%.  | Rather simplified laboratory conditions devoid of relevant in situ reservoir complexities (e.g High temperature, high pressure, presence of water). Uncertainties in NMR detection capabilities, particularly in the presence of e.g. moisture, pyrite |
| Zhao and Wang (2018) | Longmaxi shales, China | NMR-based technology on dried crushed samples                          | Fixed temperature of 25 °C. Initial equilibrium pressures of the CH <sub>4</sub> -saturated sample was ~10 MPa CO <sub>2</sub> injection pressure not specified. Final equilibrium system pressures varied between 11.8 and 12.5 MPa.  | Decreased adsorbed molar amounts of CH <sub>4</sub> due to CO <sub>2</sub> injection. They suggested the inclusion of secondary stimulating (e.g. hydraulic fracturing) methods in the design of shale CO <sub>2</sub> injection since the CH <sub>4</sub> was predominantly restricted to the pore centre after desorption by CO <sub>2</sub> exchange. |  |

plugs have also been reported in the literature (Wollenweber et al., 2009; Battistutta et al., 2010). The extent to which these changes could influence storage integrity needs further investigation. Available data (Angeli et al., 2009; Busch et al., 2010; Wollenweber et al., 2010; Edlmann et al., 2013) indicates shale cap rocks to be adequately resilient towards CO<sub>2</sub> leakage and demonstrates an encouraging note for the sequestration of CO<sub>2</sub> in gas shale systems.

As seen, production and enhanced recovery of gas from shales is a complex process. Sorption is a central mechanism in this interplay. Despite this complexity, promising results have been achieved at lab and field scales (Louk et al., 2017) and CO<sub>2</sub> injection for EGR is becoming a better understood process.

## 8. Conclusions

- Both CH<sub>4</sub> and CO<sub>2</sub> exist in critical thermodynamical state for most relevant reservoir conditions. CH<sub>4</sub> sorption increases monotonously with pressure from pressures near ambient to reservoir and can in most cases be described by a Langmuir isotherm. CO<sub>2</sub> however changes sorption behavior at the critical pressure. At lower pressures, the sorption increases monotonously, while near the critical pressure a peak in adsorption is reached and desorption occurs with increased pressure. This is not captured in low pressure experiments and standard isotherm models, e.g. multicomponent Langmuir models, are not sufficient. Extended isotherms or PVT-relations that treat both the gas and sorbed phases accurately should be applied.
- CH<sub>4</sub> and CO<sub>2</sub> adsorption storage capacity have a strong positive correlation with Total Organic Carbon, where a greater capacity is measured for CO<sub>2</sub>.
- More mature shales tend to have higher storage capacity, but also lower Langmuir pressure indicating that the gas desorbs less easily on pressure reduction.
- Kerogen type also influences storage capacity of CH<sub>4</sub> with capacity trend as Type III > Type II > Type I. More experimental data is suggested to fully support this trend. Especially, there seems to be little or no data on the correlation between CO<sub>2</sub> storage capacity and kerogen type.
- Clays can increase the storage capacity for gas adsorption, but they strongly associate with water. Measurements on dry samples are therefore likely to yield higher capacity than original state or moisture equilibrated samples.
- Adsorption is an exothermic process and the heat of adsorption for CO<sub>2</sub> is greater than for CH<sub>4</sub> in shales. CO<sub>2</sub> is therefore more favourably adsorbed. Increased temperature opposes the adsorption reaction and explains observed trends; both gases adsorb less at higher temperature.
- Recent advances have allowed NMR studies to track and distinguish gaseous and sorbed CH<sub>4</sub> and CO<sub>2</sub> in shale.

## Acknowledgments

The authors acknowledge the Research Council of Norway and the industry partners, ConocoPhillips Skandinavia AS, Aker BP ASA, Vår Energi AS, Equinor ASA, Neptune Energy Norge AS, Lundin Norway AS, Halliburton AS, Schlumberger Norge AS, and Wintershall DEA, of The National IOR Centre of Norway for support.

## References

Aljamaan, H., 2013. Petrophysical investigation on gas transport properties of the Barnett. In: Paper Presented at the SPE Annual Technical Conference and Exhibition. Ambrose, R.J., Hartman, R.C., Diaz Campos, M., Akkutlu, I.Y., Sondergeld, C., 2010. New pore-scale considerations for shale gas in place calculations. In: Paper Presented at the SPE Unconventional Gas Conference, Pittsburgh, Pennsylvania, USA.

Angeli, M., Sodal, M., Skurtveit, E., Aker, E., 2009. Experimental percolation of supercritical CO<sub>2</sub> through a caprock. Energy Procedia 1 (1), 3351–3358. <https://doi.org/10.1016/j.egypro.2009.02.123>.

Aranovich, G.L., Donohue, M.D., 1995. Adsorption isotherms for microporous adsorbents. Carbon 33 (10), 1369–1375. [https://doi.org/10.1016/0008-6223\(95\)00080-W](https://doi.org/10.1016/0008-6223(95)00080-W).

Aranovich, G.L., Donohue, M.D., 1996. Adsorption of supercritical fluids. J. Colloid Interface Sci. 180 (2), 537–541. <https://doi.org/10.1006/jcis.1996.0334>.

Aringhieri, R., 2004. Nanoporosity characteristics of some natural clay minerals and soils. Clay Clay Miner. 52 (6), 700–704. <https://doi.org/10.1346/cmn.2004.0520604>.

Aylmore, L.A.G., 1974. Gas sorption in clay mineral systems. Clay Clay Miner. 22 (2), 175–183. <https://doi.org/10.1346/cmn.1974.0220205>.

Bae, J.-S., Bhatia, S.K., 2006. High-pressure adsorption of methane and carbon dioxide on coal. Energy Fuels 20 (6), 2599–2607. <https://doi.org/10.1021/ef060318y>.

Battistutta, E., van Hemert, P., Lutynski, M., Bruining, H., Wolf, K.-H., 2010. Swelling and sorption experiments on methane, nitrogen and carbon dioxide on dry Selar Cornish coal. Int. J. Coal Geol. 84 (1), 39–48. <https://doi.org/10.1016/j.coal.2010.08.002>.

Beaton, A.P., Pawlowicz, J.G., Anderson, S.D.A., Berhane, H., Rokosh, C.D., 2010. Total Organic Carbon and Adsorption Isotherms of the Duvernay and Muskwa Formations in Alberta: Shale Gas Data Release. Energy Resources Conservation Board / Alberta Geological Survey, Edmonton, Alberta, Canada.

Bernard, S., Horsfield, B., Schulz, H.-M., Wirth, R., Schreiber, A., Sherwood, N., 2012. Geochemical evolution of organic-rich shales with increasing maturity: a STXM and TEM study of the Posidonia Shale (Lower Toarcian, northern Germany). Mar. Pet. Geol. 31 (1), 70–89. <https://doi.org/10.1016/j.marpetgeo.2011.05.010>.

Bernin, D., Hedin, N., 2018. Perspectives on NMR studies of CO<sub>2</sub> adsorption. Curr. Opin. Colloid Interface Sci. 33, 53–62. <https://doi.org/10.1016/j.cocis.2018.02.003>.

Bi, H., Jiang, Z., Li, J., Li, P., Chen, L., Pan, Q., Wu, Y., 2016. The Ono-Kondo model and an experimental study on supercritical adsorption of shale gas: a case study on Longmaxi shale in southeastern Chongqing, China. J. Nat. Gas Sci. Eng. 35, 114–121. <https://doi.org/10.1016/j.jngse.2016.08.047>.

Blok, K., Williams, R.H., Katofsky, R.E., Hendriks, C.A., 1997. Hydrogen production from natural gas, sequestration of recovered CO<sub>2</sub> in depleted gas wells and enhanced natural gas recovery. Energy 22 (2), 161–168. [https://doi.org/10.1016/S0360-5442\(96\)00136-3](https://doi.org/10.1016/S0360-5442(96)00136-3).

Bocquet, M.L., Rappe, A.M., Dai, H.L., 2005. A density functional theory study of adsorbate-induced work function change and binding energy: olefins on Ag(111). Mol. Phys. 103 (6–8), 883–890. <https://doi.org/10.1080/00268970412331333609>.

Boyer, C., Kieschnick, J., Suarez-Rivera, R., Lewis, R.E., Waters, G., 2006. Producing gas from its source. Oilfield Rev. 18 (3), 36–49.

Brunauer, S., Deming, L.S., Deming, W.E., Teller, E., 1940. On a theory of the van der Waals adsorption of gases. J. Am. Chem. Soc. 62 (7), 1723–1732. <https://doi.org/10.1021/ja01864a025>.

Bruner, K.R., Smosna, R., 2011. A Comparative Study of the Mississippian Barnett Shale, Fort Worth Basin, and Devonian Marcellus Shale, Appalachian Basin. Report to US Dept. of Energy (US DOE), National Technology Laboratory.

Burwell, R.L., 1977. Advances in Catalysis. Elsevier.

Busch, A., Krooss, B.M., Gensterblum, Y., Van Bergen, F., Pagnier, H.J.M., 2003. High-pressure adsorption of methane, carbon dioxide and their mixtures on coals with a special focus on the preferential sorption behaviour. J. Geochem. Explor. 78–79, 671–674. [https://doi.org/10.1016/S0375-6742\(03\)00122-5](https://doi.org/10.1016/S0375-6742(03)00122-5).

Busch, A., Gensterblum, Y., Krooss, B.M., Siemons, N., 2006. Investigation of high-pressure selective adsorption/desorption behaviour of CO<sub>2</sub> and CH<sub>4</sub> on coals: an experimental study. Int. J. Coal Geol. 66 (1), 53–68. <https://doi.org/10.1016/j.coal.2005.07.003>.

Busch, A., Alles, S., Gensterblum, Y., Prinz, D., Dewhurst, D.N., Raven, M.D., Stanjek, H., Krooss, B.M., 2008. Carbon dioxide storage potential of shales. Int. J. Greenh. Gas Contr. 2 (3), 297–308. <https://doi.org/10.1016/j.ijggc.2008.03.003>.

Busch, A., Alles, S., Krooss, B.M., Stanjek, H., Dewhurst, D., 2009. Effects of physical sorption and chemical reactions of CO<sub>2</sub> in shaly caprocks. Energy Procedia 1 (1), 3229–3235. <https://doi.org/10.1016/j.egypro.2009.02.107>.

Busch, A., Amann-Hildenbrand, A., Bertier, P., Waschbuesch, M., Krooss, B.M., 2010. The significance of caprock sealing integrity for CO<sub>2</sub> storage. In: Paper Presented at the SPE International Conference on CO<sub>2</sub> Capture, Storage, and Utilization, New Orleans, Louisiana, USA.

Busch, A., Gensterblum, Y., 2011. CBM and CO<sub>2</sub>-ECBM related sorption processes in coal: a review. Int. J. Coal Geol. 87 (2), 49–71. <https://doi.org/10.1016/j.coal.2011.04.011>.

Bustin, R.M., Clarkson, C.R., 1998. Geological controls on coalbed methane reservoir capacity and gas content. Int. J. Coal Geol. 38 (1–2), 3–26. [https://doi.org/10.1016/S0166-5162\(98\)00030-5](https://doi.org/10.1016/S0166-5162(98)00030-5).

Bustin, R.M., Bustin, A.M.M., Cui, A., Ross, D., Pathi, V.M., 2008. Impact of shale properties on pore structure and storage characteristics. In: Paper Presented at the SPE Shale Gas Production Conference, Fort Worth, Texas, USA.

Cancino, O.P.O., Pérez, D.P., Pozo, M., Bessieres, D., 2017. Adsorption of pure CO<sub>2</sub> and a CO<sub>2</sub>/CH<sub>4</sub> mixture on a black shale sample: manometry and microcalorimetry measurements. J. Pet. Sci. Eng. 159, 307–313. <https://doi.org/10.1016/j.petrol.2017.09.038>.

Cao, T., Song, Z., Wang, S., Cao, X., Li, Y., Xia, J., 2015. Characterizing the pore structure in the silurian and permian shales of the Sichuan Basin, China. Mar. Pet. Geol. 61, 140–150. <https://doi.org/10.1016/j.marpetgeo.2014.12.007>.

Carroll, S.A., McNab, W.W., Dai, Z., Torres, S.C., 2013. Reactivity of mount simon sandstone and the Eau Claire shale under CO<sub>2</sub> storage conditions. Environ. Sci. Technol. 47 (1), 252–261. <https://doi.org/10.1021/es301269k>.



- Cavenati, S., Grande, C.A., Rodrigues, A.E., 2004. Adsorption equilibrium of methane, carbon dioxide, and nitrogen on Zeolite 13X at high pressures. *J. Chem. Eng. Data* 49 (4), 1095–1101. <https://doi.org/10.1021/jc0498917>.
- Chalmers, G.R., Bustin, R.M., 2007. The organic matter distribution and methane capacity of the Lower Cretaceous strata of Northeastern British Columbia, Canada. *Int. J. Coal Geol.* 70 (1–3), 223–239. <https://doi.org/10.1016/j.coal.2006.05.001>.
- Chalmers, G.R., Bustin, R.M., 2008. Lower Cretaceous gas shales in northeastern British Columbia, Part I: geological controls on methane sorption capacity. *Bull. Can. Petrol. Geol.* 56 (1), 1–21. <https://doi.org/10.2113/gscpgbull.56.1.1>.
- Chang, T., Shu, Y., Ma, Y., Xu, X., Niu, Y., 2017. Isothermal adsorption and desorption properties of marine shales on Longmaxi shale in south China. *J. Nat. Gas Sci. Eng.* 7(12), 1819–1835.
- Chareonsuppanimit, P., Mohammad, S.A.R., Robert, L., Robinson, R.L., Gasem, K.A.M., 2012. High-pressure adsorption of gases on shales: measurements and modeling. *Int. J. Coal Geol.* 95, 34–46. <https://doi.org/10.1016/j.coal.2012.02.005>.
- Chareonsuppanimit, P., Mohammad, S.A., Gasem, K.A.M., 2016. Measurements and modeling of gas adsorption on shales. *Energy Fuels* 30 (3), 2309–2319. <https://doi.org/10.1021/acs.energyfuels.5b02751>.
- Chen, L., Zuo, L., Jiang, Z., Jiang, S., Liu, K., Tan, J., Zhang, L., 2019. Mechanisms of shale gas adsorption: evidence from thermodynamics and kinetics study of methane adsorption on shale. *Chem. Eng. J.* 361, 559–570. <https://doi.org/10.1016/j.cej.2018.11.185>.
- Cheng, A.-L., Huang, W.-L., 2004. Selective adsorption of hydrocarbon gases on clays and organic matter. *Org. Geochem.* 35 (4), 413–423. <https://doi.org/10.1016/j.orggeochem.2004.01.007>.
- Chikatamarla, L., Crosdale, P., 2001. Heat of methane adsorption of coal: implications for pore structure development. In: Paper Presented at the Proceedings of the International Coalbed Methane Symposium.
- Coates, G.R., Xiao, L., Prammer, M.G., 1999. NMR Logging: Principles and Applications, vol. 234. Haliburton Energy Services, Houston.
- Crosdale, P.J., 1999. Mixed methane/carbon dioxide sorption by coal: new evidence in support of pore-filling models. In: Paper Presented at the Proceedings of the 1999 International Coalbed Methane Symposium, Tuscaloosa, Alabama.
- Curtis, J.B., 2002. Fractured shale-gas systems. *AAPG Bull.* 86 (11), 1921–1938. <https://doi.org/10.1306/61eeddbe-173e-11d7-8645000102c1865d>.
- Curtis, M.E., Ambrose, R.J., Sondergeld, C.H., Rai, C.S., 2011. Investigation of the relationship between organic porosity and thermal maturity in the Marcellus Shale. In: Paper Presented at the North American Unconventional Gas Conference and Exhibition.
- Delle Piane, C., Bourdet, J., Josh, M., Clennell, M.B., Rickard, W.D., Saunders, M., Sherwood, N., Li, Z., Dewhurst, D.N., Raven, M.D., 2018. Organic matter network in post-mature Marcellus Shale: effects on petrophysical properties. *AAPG Bull.* 102 (11), 2305–2332. <https://doi.org/10.1306/04121817180>.
- Duan, S., Gu, M., Du, X., Xian, X., 2016. Adsorption equilibrium of CO<sub>2</sub> and CH<sub>4</sub> and their mixture on Sichuan Basin shale. *Energy Fuels* 30 (3), 2248–2256. <https://doi.org/10.1021/acs.energyfuels.5b02088>.
- Dubinina, M.M., 1975. Physical adsorption of gases and vapors in micropores. In: *Progress in Surface and Membrane Science*, vol. 9. Elsevier, pp. 1–70.
- Dubinina, M.M., 1980. Water vapor adsorption and the microporous structures of carbonaceous adsorbents. *Carbon* 18 (5), 355–364. [https://doi.org/10.1016/0008-6223\(80\)90007-X](https://doi.org/10.1016/0008-6223(80)90007-X).
- Eberl, D., 1984. Clay mineral formation and transformation in rocks and soils. *Philos. Trans. R. Soc. Lond. Ser. A Math. Phys. Sci.* 311 (1517), 241–257. <https://doi.org/10.1098/rsta.1984.0026>.
- Edlmann, K., Haszeldine, S., McDermott, C.I., 2013. Experimental investigation into the sealing capability of naturally fractured shale caprocks to supercritical carbon dioxide flow. *Environ. Earth Sci.* 70 (7), 3393–3409. <https://doi.org/10.1007/s12665-013-2407-y>.
- Edwards, R.W., Celia, M.A., Bandilla, K.W., Doster, F., Kanno, C.M., 2015. A model to estimate carbon dioxide injectivity and storage capacity for geological sequestration in shale gas wells. *Environ. Sci. Technol.* 49 (15), 9222–9229.
- EIA, 2013. Technically Recoverable Shale Oil and Shale Gas Resources: an Assessment of 137 Shale Formations in 41 Countries outside the United States. [https://www.eia.gov/analysis/studies/worldshalegas/archive/2013/pdf/fullreport\\_2013.pdf](https://www.eia.gov/analysis/studies/worldshalegas/archive/2013/pdf/fullreport_2013.pdf).
- Faiz, M., Aziz, N., Hutton, A., Jones, B., 1992. Porosity and gas sorption capacity of some eastern Australian coals in relation to coal rank and composition. In: Paper presented at the Coalbed Methane Symposium, Townsville.
- Fan, E., Tang, S., Zhang, C., Guo, Q., Sun, C., 2014. Methane sorption capacity of organics and clays in high-over matured shale-gas systems. *Energy Explor. Exploit.* 32 (6), 927–942. <https://doi.org/10.1260/0144-5987.32.6.927>.
- Fan, K., Li, Y., Elsworth, D., Dong, M., Yin, C., Li, Y., Chen, Z., 2018. Three stages of methane adsorption capacity affected by moisture content. *Fuel* 231, 352–360. <https://doi.org/10.1016/j.fuel.2018.05.120>.
- Fraissard, J.P., Conner, C.W., 1997. *Physical Adsorption: Experiment, Theory, and Applications*, vol. 491. Springer Science & Business Media.
- Gasparik, M., Ghanizadeh, A., Bertier, P., Gensterblum, Y., Bouw, S., Krooss, B.M., 2012. High-pressure methane sorption isotherms of black shales from The Netherlands. *Energy Fuels* 26 (8), 4995–5004. <https://doi.org/10.1021/ef300405g>.
- Gasparik, M., Bertier, P., Gensterblum, Y., Ghanizadeh, A., Krooss, B.M., Littke, R., 2014. Geological controls on the methane storage capacity in organic-rich shales. *Int. J. Coal Geol.* 123, 34–51. <https://doi.org/10.1016/j.coal.2013.06.010>.
- Glorioso, J.C., Rattia, A.J., 2012. Unconventional reservoirs: basic petrophysical concepts for shale gas. In: Paper Presented at the SPE/EAGE European Unconventional Resources Conference and Exhibition, Vienna, Austria.
- Godec, M., Koperina, G., Petrusak, R., Oudinot, A., 2013. Potential for enhanced gas recovery and CO<sub>2</sub> storage in the Marcellus Shale in the Eastern United States. *Int. J. Coal Geol.* 118, 95–104. <https://doi.org/10.1016/j.coal.2013.05.007>.
- Gumma, S., Talu, O., 2003. Gibbs dividing surface and helium adsorption. *Adsorption* 9 (1), 17–28. <https://doi.org/10.1023/a:1023859112985>.
- Guo, S., 2013. Experimental study on isothermal adsorption of methane gas on three shale samples from Upper Paleozoic strata of the Ordos Basin. *J. Pet. Sci. Eng.* 110, 132–138. <https://doi.org/10.1016/j.petrol.2013.08.048>.
- Guo, W., Xiong, W., Gao, S., Hu, Z., Liu, H., Yu, R., 2013. Impact of temperature on the isothermal adsorption/desorption of shale gas. *Pet. Explor. Dev.* 40 (4), 514–519. [https://doi.org/10.1016/S1876-3804\(13\)60066-X](https://doi.org/10.1016/S1876-3804(13)60066-X).
- Guo, W., Hu, Z., Zhang, X., Yu, R., Wang, L., 2017. Shale gas adsorption and desorption characteristics and its effects on shale permeability. *Energy Explor. Exploit.* 35 (4), 463–481. <https://doi.org/10.1177/0144598716684306>.
- Hao, F., Zou, H., Lu, Y., 2013. Mechanisms of shale gas storage: implications for shale gas exploration in China mechanisms of Shale Gas Storage. *AAPG Bull.* 97 (8), 1325–1346. <https://doi.org/10.1306/02141312091>.
- Helgeson, H.C., Richard, L., McKenzie, W.F., Norton, D.L., Schmitt, A., 2009. A chemical and thermodynamic model of oil generation in hydrocarbon source rocks. *Geochem. Cosmochim. Acta* 73 (3), 594–695. <https://doi.org/10.1016/j.gca.2008.03.004>.
- Heller, R., Zoback, M., 2014. Adsorption of methane and carbon dioxide on gas shale and pure mineral samples. *J. Unconv. Oil Gas Resour.* 8, 14–24. <https://doi.org/10.1016/j.juogr.2014.06.001>.
- Herrera, L., Fan, C., Do, D., Nicholson, D., 2011. A revisit to the Gibbs dividing surfaces and helium adsorption. *Adsorption* 17 (6), 955–965. <https://doi.org/10.1007/s10450-011-9374-y>.
- Hong, L., Jain, J., Romanov, V., Lopano, C., Disenhof, C., Goodman, A., Hedges, S., Soeder, D., Sanguinito, S., Dillmore, R., 2016. An investigation of factors affecting the interaction of CO<sub>2</sub> and CH<sub>4</sub> on shale in Appalachian Basin. *J. Unconv. Oil Gas Resour.* 14, 99–112. <https://doi.org/10.1016/j.juogr.2016.02.003>.
- Huang, L., Ning, Z., Wang, Q., Zhang, W., Cheng, Z., Wu, X., Qin, H., 2018. Effect of organic type and moisture on CO<sub>2</sub>/CH<sub>4</sub> competitive adsorption in kerogen with implications for CO<sub>2</sub> sequestration and enhanced CH<sub>4</sub> recovery. *J. Appl. Energy* 210, 28–43. <https://doi.org/10.1016/j.apenergy.2017.10.122>.
- Huo, P., Zhang, D., Yang, Z., Li, W., Zhang, J., Jia, S., 2017. CO<sub>2</sub> geological sequestration: displacement behavior of shale gas methane by carbon dioxide injection. *Int. J. Greenh. Gas Contr.* 66, 48–59. <https://doi.org/10.1016/j.ijggc.2017.09.001>.
- Iijima, M., Nagayasu, T., Kamiyo, T., Nakatani, S., 2011. MHI's energy efficient flue gas CO<sub>2</sub> capture technology and large scale ccs demonstration test at coal-fired power plants in USA. *Mitsubishi Heavy Ind. Tech. Rev.* 48 (1), 26–32. <https://www.mhi.co.jp/technology/review/pdf/e481/e481026.pdf>.
- Inglezakis, V.J., Zorpas, A.A., 2012. Heat of adsorption, adsorption energy and activation energy in adsorption and ion exchange systems. *Desalination Water Treat.* 39 (1–3), 149–157. <https://doi.org/10.5004/dwt.2012.3000>.
- Jarvie, D.M., Claxton, B.L., Henk, F., TBJ, 2001. Oil and shale gas from the Barnett shale, Ft. Worth basin, Texas. In: Paper Presented at the AAPG Annual Meeting Program.
- Jarvie, D.M., Hill, R.J., Ruble, T.E., Pollastro, R.M., 2007. Unconventional shale-gas systems: the Mississippian Barnett Shale of north-central Texas as one model for thermogenic shale-gas assessment. *AAPG Bull.* 91 (4), 475–499. <https://doi.org/10.1306/12190606068>.
- Ji, L., Zhang, T., Milliken, K.L., Qu, J., Zhang, X., 2012. Experimental investigation of main controls to methane adsorption in clay-rich rocks. *Appl. Geochem.* 27 (12), 2533–2545. <https://doi.org/10.1016/j.apgeochem.2012.08.027>.
- Jia, B., Tsau, J.-S., Barati, R., 2018. Different flow behaviors of low-pressure and high-pressure carbon dioxide in shales. *SPE J.* 23 (04), 1452–1468. <https://doi.org/10.2118/191121-pa>.
- Jiang, Y., Luo, Y., Lu, Y., Qin, C., Liu, H., 2016. Effects of supercritical CO<sub>2</sub> treatment time, pressure, and temperature on microstructure of shale. *Energy* 97, 173–181. <https://doi.org/10.1016/j.energy.2015.12.124>.
- Jin, X., Wang, X., Liu, X., Jiao, H., Sun, L., Su, L., Bi, L., Chen, Y., 2017. Low field cryoporometry NMR for mesopores distribution in shale. In: Paper Presented at the SPE/IATMI Asia Pacific Oil & Gas Conference and Exhibition, Jakarta, Indonesia.
- Kalkreuth, W., Holz, M., Levandowski, J., Kern, M., Casagrande, J., Weniger, P., Krooss, B., 2013. The coalbed methane (CBM) potential and CO<sub>2</sub> storage capacity of the santa Terezinha coalfield, Paraná Basin, Brazil—3D modelling, and coal and carbonaceous shale characteristics and related desorption and adsorption capacities in samples from exploration Borehole CBM001-ST-RS. *Energy Explor. Exploit.* 31 (4), 485–527. <https://doi.org/10.1260/0144-5987.31.4.485>.
- Kang, S.M., Fathi, E., Ambrose, R.J., Akkutlu, I.Y., Sigal, R.F., 2011. Carbon dioxide storage capacity of organic-rich shales. *SPE J.* 16 (04), 842–855. <https://doi.org/10.2118/134583-pa>.
- Karacan, C.Ö., Mitchell, G.D., 2003. Behavior and effect of different coal microlithotypes during gas transport for carbon dioxide sequestration into coal seams. *Int. J. Coal Geol.* 53 (4), 201–217. [https://doi.org/10.1016/s0166-5162\(03\)00030-2](https://doi.org/10.1016/s0166-5162(03)00030-2).
- Khosrokhavar, R., 2015. Sorption of CH<sub>4</sub> and CO<sub>2</sub> on Belgium carboniferous shale using a manometric set-up. In: *Mechanisms for CO<sub>2</sub> Sequestration in Geological Formations and Enhanced Gas Recovery*. Springer International Publishing, pp. 49–66.
- Krooss, B.M., Littke, R., Müller, B., Frielingsdorf, J., Schwochau, K., Idiz, E.F., 1995. Generation of nitrogen and methane from sedimentary organic matter: implications on the dynamics of natural gas accumulations. *Chem. Geol.* 126 (3), 291–318. [https://doi.org/10.1016/0009-2541\(95\)00124-7](https://doi.org/10.1016/0009-2541(95)00124-7).
- Kus, J., Araujo, C.V., Borrego, A.G., Flores, D., Hackley, P.C., Hámor-Vidó, M., Kalaitzidis, S., Kommeren, C.J., Kwiecińska, B., Mastalerz, M., Mendonça Filho, J.G., Menezes, T.R., Misz-Kennan, M., Nowak, G.J., Petersen, H.L., Rallakis, D., Suárez-Ruiz, I., Šýkorová, I., Životić, D., 2017. Identification of alginite and bituminite in rocks other than coal. 2006, 2009, and 2011 round robin exercises of the ICCP

- Identification of Dispersed Organic Matter Working Group. *Int. J. Coal Geol.* 178, 26–38. <https://doi.org/10.1016/j.coal.2017.04.013>.
- Lancaster, D., Hill, D., 1993. A multi-laboratory comparison of isotherm measurements of Antrim shale samples. In: Paper Presented at the SCA Conference, Otsego County, Michigan.
- Lane, H., Watson, A., Lancaster, D., 1989. Identifying and estimating desorption from Devonian shale gas production data. In: Paper Presented at the SPE Annual Technical Conference and Exhibition.
- Langmuir, I., 1916. Langmuir, I., 1916. The constitution and fundamental properties of solids and liquids: Part I, Solids. *J. Am. Chem. Soc.* 38 (11), 2221–2295. <https://doi.org/10.1021/ja02268a002>.
- Langmuir, I., 1918. The adsorption of gases on plane surfaces of glass, mica and platinum. *J. Am. Chem. Soc.* 40 (9), 1361–1403. <https://doi.org/10.1021/ja02242a004>.
- Li, A., Ding, W., Zhou, X., Cao, X., Zhang, M., Fu, F., Chen, E., 2017. Investigation of the methane adsorption characteristics of marine shale: a case study of lower cambrian Qiongzhusi shale in eastern Yunnan province, south China. *Energy Fuels* 31 (3), 2625–2635. <https://doi.org/10.1021/acs.energyfuels.6b03168>.
- Liu, D., Li, Y., Yang, S., Agarwal, R.K., 2019. CO<sub>2</sub> sequestration with enhanced shale gas recovery. *Energy Sources, Part A Recovery, Util. Environ. Eff.* 1–11. <https://doi.org/10.1080/15567036.2019.1587069>.
- Liu, F., Lu, P., Griffith, C., Hedges, S.W., Soong, Y., Hellevang, H., Zhu, C., 2012. CO<sub>2</sub>-brine-caprock interaction: reactivity experiments on Eau Claire shale and a review of relevant literature. *Int. J. Greenh. Gas Contr.* 7, 153–167. <https://doi.org/10.1016/j.ijggc.2012.01.012>.
- Liu, J., Yao, Y., Liu, D., Elsworth, D., 2017. Experimental evaluation of CO<sub>2</sub> enhanced recovery of adsorbed-gas from shale. *Int. J. Coal Geol.* 179, 211–218. <https://doi.org/10.1016/j.coal.2017.06.006>.
- Liu, Y., Li, H.A., Tian, Y., Jin, Z., Deng, H., 2018. Determination of the absolute adsorption/desorption isotherms of CH<sub>4</sub> and n-C<sub>4</sub>H<sub>10</sub> on shale from a nano-scale perspective. *Fuel* 218, 67–77. <https://doi.org/10.1016/j.fuel.2018.01.012>.
- Loucks, R.G., Reed, R.M., Ruppel, S.C., Hammes, U., 2012. Spectrum of pore types and networks in mudrocks and a descriptive classification for matrix-related mudrock pores. *AAPG Bull.* 96 (6), 1071–1098. <https://doi.org/10.1306/08171111061>.
- Loucks, R.G., Reed, R.M., Ruppel, S.C., Jarvie, D.M., 2009. Morphology, genesis, and distribution of nanometer-scale pores in siliceous mudstones of the mississippian Barnett shale. *J. Sediment. Res.* 79 (12) <https://doi.org/10.2110/jsr.2009.092.1527-1404>.
- Louk, K., Rippei, N., Luxbacher, K., Gilliland, E., Tang, X., Keles, C., Schlosser, C., Diminick, E., Keim, S., Amante, J., Michael, K., 2017. Monitoring CO<sub>2</sub> storage and enhanced gas recovery in unconventional shale reservoirs: results from the Morgan County, Tennessee injection test. *J. Nat. Gas Sci. Eng.* 45, 11–25. <https://doi.org/10.1016/j.jngse.2017.03.025>.
- Lu, X.C., Li, F.C., Watson, A.T., 1995. Adsorption studies of natural gas storage in Devonian shales. *SPE Form. Eval.* 10 (02), 109–113. <https://doi.org/10.2118/26632-pa>.
- Lu, Y., Ao, X., Tang, J., Jia, Y., Zhang, X., Chen, Y., 2016. Swelling of shale in supercritical carbon dioxide. *J. Nat. Gas Sci. Eng.* 30, 268–275. <https://doi.org/10.1016/j.jngse.2016.02.011>.
- Luo, X., Wang, S., Wang, Z., Jing, Z., Lv, M., Zhai, Z., Han, T., 2015. Adsorption of methane, carbon dioxide and their binary mixtures on Jurassic shale from the Qaidam Basin in China. *Int. J. Coal Geol.* 150–151, 210–223. <https://doi.org/10.1016/j.coal.2015.09.004>.
- Lutyński, M., Waszczuk, P., Słomski, P., Szczepański, J., 2017. CO<sub>2</sub> sorption of Pomeranian gas bearing shales – the effect of clay minerals. *Energy Procedia* 125, 457–466. <https://doi.org/10.1016/j.egypro.2017.08.153>.
- Lyu, Q., Long, X., Ranjith, P.G., Kang, Y., 2016. Unconventional gas: experimental study of the influence of subcritical carbon dioxide on the mechanical properties of black shale. *Energies* 9 (7), 516. <https://doi.org/10.3390/en9070516>.
- Lyu, Q., Ranjith, P.G., Long, X., Ji, B., 2016. Experimental investigation of mechanical properties of black shales after CO<sub>2</sub>-water-rock interaction. *Materials* 9 (8), 663. <https://doi.org/10.20944/preprints201608.0056.v1>.
- Lyu, Q., Long, X., Ranjith, P., Tan, J., Zhou, J., Wang, Z., Luo, W., 2018. A laboratory study of geomechanical characteristics of black shales after sub-critical/super-critical CO<sub>2</sub> + brine saturation. *Geomech. Geophys. Geo-Energy Geo-Resour.* 1–16. <https://doi.org/10.1007/s40948-018-0079-5>.
- Lyu, Q., Long, X., Ranjith, P.G., Tan, J., Kang, Y., Wang, Z., 2018. Experimental investigation on the mechanical properties of a low-clay shale with different adsorption times in sub-/super-critical CO<sub>2</sub>. *Energy* 147, 1288–1298. <https://doi.org/10.1016/j.energy.2018.01.084>.
- Ma, Y., Zhong, N., Li, D., Pan, Z., Cheng, L., Liu, K., 2015. Organic matter/clay mineral intergranular pores in the Lower Cambrian Lujiaoping Shale in the north-eastern part of the upper Yangtze area, China: a possible microscopic mechanism for gas preservation. *Int. J. Coal Geol.* 137, 38–54. <https://doi.org/10.1016/j.coal.2014.11.001>.
- Ma, Y., Yue, C., Li, S., Xu, X., Niu, Y., 2018. Study of CH<sub>4</sub> and CO<sub>2</sub> competitive adsorption on shale in Yibin, sichuan province of China. *Carbon Resour. Convers.* <https://doi.org/10.1016/j.crccon.2018.11.005>.
- Majewska, Z., Ceglarska-Stefańska, G., Majewski, S., Ziętek, J., 2009. Binary gas sorption/desorption experiments on a bituminous coal: simultaneous measurements on sorption kinetics, volumetric strain and acoustic emission. *Int. J. Coal Geol.* 77 (1), 90–102. <https://doi.org/10.1016/j.coal.2008.09.009>.
- Malbrunot, P., Vidal, D., Vermesse, J., Chahine, R., Bose, T.K., 1997. Adsorbent helium density measurement and its effect on adsorption isotherms at high pressure. *Langmuir* 13 (3), 539–544. <https://doi.org/10.1021/la950969e>.
- Manger, K.C., Oliver, S.J.P., Curtis, J., B, Scheper, R.J., 1991. Geologic influences on the location and production of Antrim shale gas, Michigan Basin. In: Paper Presented at the Low Permeability Reservoirs Symposium.
- Manz, B., Gladden, L.F., Warren, P.B., 1999. Flow and dispersion in porous media: Lattice-Boltzmann and NMR studies. *AIChE J.* 45 (9), 1845–1854. <https://doi.org/10.1002/aic.690450902>.
- Mendhe, V.A., Mishra, S., Varma, A.K., Kamble, A.D., Bannerjee, M., Sutay, T., 2017. Gas reservoir characteristics of the lower gondwana shales in Raniganj basin of eastern India. *J. Pet. Sci. Eng.* 149, 649–664. <https://doi.org/10.1016/j.petrol.2016.11.008>.
- Menon, P.G., 1968. Adsorption at high pressures. *Chem. Rev.* 68 (3), 277–294. <https://pubs.acs.org/doi/abs/10.1021/cr60253a002>.
- Merey, S., Sinayuc, C., 2016. Analysis of carbon dioxide sequestration in shale gas reservoirs by using experimental adsorption data and adsorption models. *J. Nat. Gas Sci. Eng.* 36, 1087–1105. <https://doi.org/10.1016/j.jngse.2016.02.052>.
- Merey, S., Sinayuc, C., 2018. Adsorption behaviour of shale gas reservoirs. *Int. J. Oil Gas Coal Technol.* 17, 172. <https://doi.org/10.1504/ijogct.2018.089941>.
- Merkel, A., Fink, R., Littke, R., 2015. The role of pre-adsorbed water on methane sorption capacity of Bossier and Haynesville shales. *Int. J. Coal Geol.* 147–148, 1–8. <https://doi.org/10.1016/j.coal.2015.06.003>.
- Milliken, K.L., Rudnicki, M., Awwiller, D.N., Zhang, T., 2013. Organic matter-hosted pore system, Marcellus formation (Devonian), Pennsylvania Geohorizon. *AAPG Bull.* 97 (2), 177–200. <https://doi.org/10.1306/07231212048>.
- Moffat, D.H., Weale, K.E., 1955. Sorption by coal of methane at high pressures, 34 (4), 449–462.
- Mullen, J., 2010. Petrophysical characterization of the Eagle Ford shale in south Texas. In: Paper Presented at the Canadian Unconventional Resources and International Petroleum Conference, Calgary, Alberta, Canada.
- Murata, K., El-Merrauui, M., Kaneko, K., 2001. A new determination method of absolute adsorption isotherm of supercritical gases under high pressure with a special relevance to density-functional theory study. *J. Chem. Phys.* 114 (9), 4196–4205. <https://doi.org/10.1063/1.1344926>.
- Neimark, A.V., Ravikovitch, P.I., 1997. Calibration of pore volume in adsorption experiments and theoretical models. *Langmuir* 13 (19), 5148–5160. <https://doi.org/10.1021/la970266s>.
- Nelson, P.H., 2009. Pore-throat sizes in sandstones, tight sandstones, and shales. *AAPG Bull.* 93 (3), 329–340. <https://doi.org/10.1306/10240808059>.
- Nuttal, B.C., Eble, C., Bustin, R.M., Drahozal, J.A., 2003. Analysis of Devonian Black Shales in Kentucky for Potential Carbon Dioxide Sequestration and Enhanced Natural Gas Production. UNT Libraries Government Documents Department. [digital.library.unt.edu/ark:/67531/metadc786289/](https://doi.org/10.2110/jsr.2009.092.1527-1404).
- Nuttal, B.C., Eble, C., Bustin, R.M., Drahozal, J.A., 2005. Analysis of Devonian black shales in Kentucky for potential carbon dioxide sequestration and enhanced natural gas production. In: *Greenhouse Gas Control Technologies*, vol. 7. Elsevier, pp. 2225–2228.
- Oldenburg, C.M., Pruess, K., Benson, S.M., Fuels, 2001. Process modeling of CO<sub>2</sub> injection into natural gas reservoirs for carbon sequestration and enhanced gas recovery. *Energy Fuels* 15 (2), 293–298. <https://doi.org/10.1021/e000247h>.
- Passy, Q.R., Bohacs, K., Esch, W.L., Klimentidis, R., Sinha, S., 2010. From oil-prone source rock to gas-producing shale reservoir-geologic and petrophysical characterization of unconventional shale gas reservoirs. In: Paper Presented at the International Oil and Gas Conference and Exhibition in China.
- Pei, P., Ling, K., He, J., Liu, Z., 2015. Shale gas reservoir treatment by a CO<sub>2</sub>-based technology. *J. Nat. Gas Sci. Eng.* 26, 1595–1606. <https://doi.org/10.1016/j.jngse.2015.03.026>.
- Pino, D., Plantier, F., Bessieres, D., 2014. Experimental determination of the adsorption isotherms in gas mixtures under extended pressure and temperature range. *J. Therm. Anal. Calorim.* 117 (3), 1469–1477. <https://doi.org/10.1007/s10973-014-3931-z>.
- Polanyi, M., 1932. Section III.—theories of the adsorption of gases. A general survey and some additional remarks. Introductory paper to section III. *Trans. Faraday Soc.* 28, 316–333. <https://doi.org/10.1039/TF9322800316>.
- Pozo, M., Pino, D., Bessieres, D., 2017. Effect of thermal events on maturation and methane adsorption of Silurian black shales (Checa, Spain). *Appl. Clay Sci.* 136, 208–218. <https://doi.org/10.1016/j.clay.2016.11.026>.
- Pusch, A.-K., Splith, T., Moschkowitz, L., Karmakar, S., Biniwale, R., Sant, M., Suffritti, G. B., Demontis, P., Cravillon, J., Pantatosaki, E.J.A., 2012. NMR studies of carbon dioxide and methane self-diffusion in ZIF-8 at elevated gas pressures. *J. Phys. Chem. C* 116 (5), 359–366.
- Pytte, A.M., Reynolds, R.C., 1989. The thermal transformation of smectite to illite. In: *Thermal History of Sedimentary Basins*. Springer, pp. 133–140.
- Ramos, S., 2004. The Effect of Shale Composition on the Gas Sorption Potential of Organic-Rich Mudrocks in the Western Canadian Sedimentary Basin. University of British Columbia. Retrieved from.
- Rani, S., Padmanabhan, E., Prusty, B.K., 2019. Review of gas adsorption in shales for enhanced methane recovery and CO<sub>2</sub> storage. *J. Pet. Sci. Eng.* 175, 634–643. <https://doi.org/10.1016/j.petrol.2018.12.081>.
- Rassenfoss, S., 2017. Shale EOR works, but will it make a difference? SPE-1017-0034-JPT 69 (10), 34–40. <https://doi.org/10.2118/1017-0034-JPT>.
- Regan, M., 2007. A Review of the Potential for Carbon Dioxide (CO<sub>2</sub>) Enhanced Gas Recovery in Australia.
- Rexer, T.F., Mathia, E.J., Aplin, A.C., Thomas, K.M., 2014. High-pressure methane adsorption and characterization of pores in Posidonia shales and isolated kerogens. *Energy Fuels* 28 (5), 2886–2901. <https://doi.org/10.1021/ef402466m>.
- Rice, D.D., Law, B.E., Clayton, J.L., 1993. Coalbed gas: an undeveloped resource. *U. S. Geol. Surv. Prof. Pap.* 1570, 389–404.

- Ross, D.J.K., Bustin, R.M., 2007. Shale gas potential of the lower Jurassic Gordondale member, northeastern British Columbia, Canada. *Bull. Can. Petrol. Geol.* 55 (1), 51–75. <https://doi.org/10.2113/gscpgbull.55.1.51>.
- Ross, D.J.K., Bustin, R.M., 2007. Impact of mass balance calculations on adsorption capacities in microporous shale gas reservoirs. *Fuel* 86 (17), 2696–2706. <https://doi.org/10.1016/j.fuel.2007.02.036>.
- Ross, D.J.K., Bustin, R.M., 2008. Characterizing the shale gas resource potential of Devonian–Mississippian strata in the Western Canada sedimentary basin: application of an integrated formation evaluation. *AAPG Bull.* 92 (1), 87–125. <https://doi.org/10.1306/09040707048>.
- Ross, D.J.K., Bustin, R.M., 2009. The importance of shale composition and pore structure upon gas storage potential of shale gas reservoirs. *Mar. Pet. Geol.* 26 (6), 916–927. <https://doi.org/10.1016/j.marpetgeo.2008.06.004>.
- Rudzinski, W., Everett, D.H., 2012. *Adsorption of Gases on Heterogeneous Surfaces*. Academic Press.
- Ruppel, S., Loucks, R., 2008. Black mudrocks: lessons and questions from the mississippian Barnett shale in the southern midcontinent. *Sediment. Rec.* 6 (2), 4–8. <https://doi.org/10.2110/sedred.2008.2.4>.
- Saha, P., Chowdhury, S., 2011. Insight into adsorption thermodynamics. In: *Thermodynamics*. InTechOpen.
- Scaranto, J., Mallia, G., Harrison, N.M., 2011. An efficient method for computing the binding energy of an adsorbed molecule within a periodic approach. The application to vinyl fluoride at rutile TiO<sub>2</sub>(110) surface. *Comput. Mater. Sci.* 50 (7), 2080–2086. <https://doi.org/10.1016/j.commatsci.2011.02.011>.
- Schaefer, H.T., Glezakou, V.-A., Owen, A.T., Ramprasad, S., Martin, P.F., McGrail, B.P., 2013. Surface condensation of CO<sub>2</sub> onto kaolinite. *Environ. Sci. Technol. Lett.* 1 (2), 142–145. <https://doi.org/10.1021/ez400169b>.
- Schaefer, H.T., Davidson, C.L., Owen, A.T., Miller, Q.R., Loring, J.S., Thompson, C.J., Bacon, D.H., Glezakou, V.A., McGrail, B.P., 2014. CO<sub>2</sub> utilization and storage in shale gas reservoirs: experimental results and economic impacts. *Energy Procedia* 63, 7844–7851. <https://doi.org/10.1016/j.egypro.2014.11.819>. PNNL-SA-105772).
- Schettler Jr., P., Parmely, C., 1990. The measurement of gas desorption isotherms for Devonian shale. *GRI Devonian Gas Shale Technol. Rev.* 7 (1), 4–9.
- Schettler Jr., P., Parmely, C., 1991. Contributions to total storage capacity in Devonian shales. In: *Paper Presented at the SPE Eastern Regional Meeting*.
- Schieber, J., 2010. Common themes in the formation and preservation of intrinsic porosity in shales and mudstones - illustrated with examples across the phanerozoic. In: *Paper Presented at the SPE Unconventional Gas Conference*.
- Seewald, J.S., 2003. Organic–inorganic interactions in petroleum-producing sedimentary basins. *Nature* 426, 327. <https://doi.org/10.1038/nature02132>.
- Sharma, G., Galvis-Portilla, H., 2018. Impact of total organic carbon on adsorption capacity, in-place hydrocarbons, and ultimate recovery: a case study of the duvernay formation in alberta, Canada. In: *Paper Presented at the Abu Dhabi International Petroleum Exhibition & Conference*.
- Sing, K.S.W., Everett, D.H., Haul, R.A.W., Moscou, L., Pierotti, L.A., Rouquerol, J., Siemieniowska, T., 1985. International union of pure and applied chemistry physical chemistry division reporting physisorption data for gas/soils systems with special reference to the determination of surface area and porosity. *Pure Appl. Chem.* 57, 603–619. <https://doi.org/10.1515/iupac.54.0530>.
- Sircar, S., 1985. Excess properties and thermodynamics of multicomponent gas adsorption. *J. Chem. Soc., Faraday Trans. 1: Phys. Chem. Condens. Phases* 81 (7), 1527–1540. <https://doi.org/10.1039/F19858101527>.
- Slatt, R.M., O'Brien, N.R., 2011. Pore types in the Barnett and Woodford gas shales: understanding gas storage and migration pathways in fine-grained rocks geohorizon. *AAPG Bull.* 95 (12), 2017–2030. <https://doi.org/10.1306/03301110145>.
- Soeder, D.J., 1988. Porosity and permeability of eastern Devonian gas shale. *SPE Form. Eval.* 3 (01), 116–124. <https://doi.org/10.2118/15213-PA>.
- Sondergeld, C.H., Ambrose, R.J., Rai, C.S., Moncrieff, J., 2010. *Micro-structural studies of gas shales*. In: *Paper Presented at the SPE Unconventional Gas Conference*.
- Steele, W.A., 1974. *The Interaction of Gases with Solid Surfaces*. Pergamon, Oxford.
- Stoeckli, H.F., 1990. Microporous carbons and their characterization: the present state of the art. *Carbon* 28 (1), 1–6. [https://doi.org/10.1016/0008-6223\(90\)90086-E](https://doi.org/10.1016/0008-6223(90)90086-E).
- Strapoc, D., Mastalerz, M., Schimmelmann, A., Drobniak, A., Hasenmueller, N.R., 2010. Geochemical constraints on the origin and volume of gas in the new Albany shale (Devonian–Mississippian), eastern Illinois basin. *AAPG Bull.* 94 (11), 1713–1740. <https://doi.org/10.1306/06301009197>.
- Strubinger, J.R., Song, H., Patcher, J.F., 1991. High-pressure phase distribution isotherms for supercritical fluid chromatographic systems. 1. Pure carbon dioxide. *Anal. Chem.* 63 (2), 98–103. <https://doi.org/10.1021/ac00002a003>.
- Sudibandriyo, M., Pan, Z., Fitzgerald, J.E., Robinson, R.L., Gasem, K.A.M., 2003. Adsorption of methane, nitrogen, carbon dioxide, and their binary mixtures on dry activated carbon at 318.2 K and pressures up to 13.6 MPa. *Langmuir* 19 (13), 5323–5331. <https://doi.org/10.1021/la020976k>.
- Sucha, V., Šrodoň, J., Clauer, N., Elsass, F., Eberl, D., Kraus, I., Madejová, J., 2001. Weathering of smectite and illite-smectite under temperate climatic conditions. *Clay Miner.* 36 (3), 403–419. <https://doi.org/10.1180/000985501750539490>.
- Teichmüller, M., 1971. Anwendung kohlenpetrographischer Methoden bei der Erdöl-und Erdgasprospektion. *Erdöl Kohle* 24, 69–76.
- Tan, J., Weniger, P., Krooss, B., Merkel, A., Horsfield, B., Zhang, J., Boreham, C.J., van Graas, G., Tocher, B.A., 2014. Shale gas potential of the major marine shale formations in the Upper Yangtze Platform, South China, Part II: methane sorption capacity. *Fuel* 129, 204–218. <https://doi.org/10.1016/j.fuel.2014.03.064>.
- Tang, X., Rippepi, N., Luxbacher, K., Pitcher, E., 2017. Adsorption models for methane in shales: review, comparison, and application. *Energy Fuels* 31 (10), 10787–10801. <https://doi.org/10.1021/acs.energyfuels.7b01948>.
- Tang, S., Zhang, J., Elsworth, D., Tang, X., Li, Z., Du, X., Yang, X., 2016. Lithofacies and pore characterization of the lower permian shanxi and Taiyuan shales in the southern north China basin. *J. Nat. Gas Sci. Eng.* 36, 644–661. <https://doi.org/10.1016/j.jngse.2016.11.013>.
- Tao, Z., Bielicki, J.M., Clarens, A.F., 2014. Physicochemical factors impacting CO<sub>2</sub> sequestration in depleted shale formations: the case of the Utica shale. *Energy Procedia* 63, 5153–5163. <https://doi.org/10.1016/j.egypro.2014.11.545>.
- Thommes, M., 2010. Physical adsorption characterization of nanoporous materials. *Chem. Ing. Tech.* 82 (7), 1059–1073. <https://doi.org/10.1002/cite.201000064>.
- Tissot, B.P., Welte, D.H., 1984. *Petroleum formation and occurrence*. In: Springer-Verlag, Berlin-Heidelberg.
- Vandenbroucke, M., Largeau, C., 2007. Kerogen origin, evolution and structure. *Org. Geochem.* 38 (5), 719–833. <https://doi.org/10.1016/j.orggeochem.2007.01.001>.
- Wang, H., Li, G., Shen, Z., 2012. A feasibility analysis on shale gas exploitation with supercritical carbon dioxide. *Energy Sources, Part A Recovery, Util. Environ. Eff.* 34 (15), 1426–1435. <https://doi.org/10.1080/15567036.2010.529570>.
- Wang, L., Yu, Q., 2016. The effect of moisture on the methane adsorption capacity of shales: a study case in the eastern Qaidam Basin in China. *J. Hydrol.* 542, 487–505. <https://doi.org/10.1016/j.jhydrol.2016.09.018>.
- Wang, S., Song, Z., Cao, T., Song, X., 2013. The methane sorption capacity of Paleozoic shales from the Sichuan Basin, China. *Mar. Pet. Geol.* 44, 112–119. <https://doi.org/10.1016/j.marpetgeo.2013.03.007>.
- Wang, Y., Zhu, Y., Liu, S., Zhang, R., 2016. Methane adsorption measurements and modeling for organic-rich marine shale samples. *Fuel* 172, 301–309. <https://doi.org/10.1016/j.fuel.2015.12.074>.
- Venaruzzo, J.L., Volzone, C., Rueda, M.L., Ortega, J., 2002. Modified bentonitic clay minerals as adsorbents of CO, CO<sub>2</sub> and SO<sub>2</sub> gases. *Microporous Mesoporous Mater.* 56 (1), 73–80. [https://doi.org/10.1016/S1387-1811\(02\)00443-2](https://doi.org/10.1016/S1387-1811(02)00443-2).
- Wang, Z., Krupnick, A., 2015. A retrospective review of shale gas development in the United States: what led to the boom? *Econ. Energy Environ. Pol.* 4 (1), 5–18. <https://doi.org/10.2139/ssrn.2286239>.
- Wei, X., Wei, G., Honglin, L., Shusheng, G., Zhiming, H., Farong, Y., 2012. Shale reservoir characteristics and isothermal adsorption properties. *Nat. Gas. Ind.* 32 (1), 113–116.
- Weniger, P., Kalkreuth, W., Busch, A., Krooss, B.M., 2010. High-pressure methane and carbon dioxide sorption on coal and shale samples from the Paraná Basin, Brazil. *J. Int. J. Coal Geol.* 84 (3–4), 190–205. <https://doi.org/10.1016/j.coal.2010.08.003>.
- Wollenweber, J., Alles, S., Kronimus, A., Busch, A., Stanjek, H., Krooss, B.M., 2009. Caprock and overburden processes in geological CO<sub>2</sub> storage: an experimental study on sealing efficiency and mineral alterations. *Energy Procedia* 1 (1), 3469–3476. <https://doi.org/10.1016/j.egypro.2009.02.138>.
- Wollenweber, J., Alles, S., Busch, A., Krooss, B.M., Stanjek, H., Littke, R., 2010. Experimental investigation of the CO<sub>2</sub> sealing efficiency of caprocks. *Int. J. Greenh. Gas Contr.* 4 (2), 231–241. <https://doi.org/10.1016/j.ijggc.2010.01.003>.
- Wu, C., Tuo, J., Zhang, L., Zhang, M., Li, J., Liu, Y., Qian, Y., 2017. Pore characteristics differences between clay-rich and clay-poor shales of the Lower Cambrian Niutitang Formation in the Northern Guizhou area, and insights into shale gas storage mechanisms. *Int. J. Coal Geol.* 178, 13–25. <https://doi.org/10.1016/j.coal.2017.04.009>.
- Xia, J., Song, Z., Wang, S., Zeng, W., 2017. Preliminary study of pore structure and methane sorption capacity of the Lower Cambrian shales from the north Gui-zhou Province. *J. Nat. Gas Sci. Eng.* 38, 81–93. <https://doi.org/10.1016/j.jngse.2016.12.021>.
- Xiong, J., Liu, X., Liang, L., Zeng, Q., 2017. Adsorption of methane in organic-rich shale nanopores: an experimental and molecular simulation study. *Fuel* 200, 299–315. <https://doi.org/10.1016/j.fuel.2017.03.083>.
- Yang, F., Xie, C., Ning, Z., Krooss, B., 2016. High-pressure methane sorption on dry and moisture-equilibrated shales. *Energy Fuels* 31 (1), 482–492. <https://doi.org/10.1021/acs.energyfuels.6b02999>.
- Yin, H., Zhou, J., Jiang, Y., Xian, X., Liu, Q., 2016. Physical and structural changes in shale associated with supercritical CO<sub>2</sub> exposure. *Fuel* 184, 289–303. <https://doi.org/10.1016/j.fuel.2016.07.028>.
- Yin, H., Zhou, J., Xian, X., Jiang, Y., Lu, Z., Tan, J., Liu, G., 2017. Experimental study of the effects of sub- and super-critical CO<sub>2</sub> saturation on the mechanical characteristics of organic-rich shales. *Energy* 132, 84–95. <https://doi.org/10.1016/j.energy.2017.05.064>.
- Yin, T., Liu, D., Cai, Y., Zhou, Y., Yao, Y., 2017. Size distribution and fractal characteristics of coal pores through nuclear magnetic resonance cryoporometry. *Energy Fuels* 31 (8), 7746–7757. <https://doi.org/10.1021/acs.energyfuels.7b00389>.
- Yuan, W., Pan, Z., Li, X., Yang, Y., Zhao, C., Connell, L.D., Li, S., He, J., 2014. Experimental study and modelling of methane adsorption and diffusion in shale, 117, 509–519.
- Zhang, T., Ellis, G.S., Ruppel, S.C., Milliken, K., Yang, R., 2012. Effect of organic-matter type and thermal maturity on methane adsorption in shale-gas systems, 47, 120–131.
- Zhao, G., Wang, C., 2018. Influence of CO<sub>2</sub> on the adsorption of CH<sub>4</sub> on shale using low-field nuclear magnetic resonance technique. *Fuel* 238, 51–58. <https://doi.org/10.1016/j.fuel.2018.10.092>.
- Zheng, X., Zhang, B., Saneji, H., Bao, H., Meng, Z., Wang, C., Li, K., 2018. Pore structure characteristics and its effect on shale gas adsorption and desorption behavior. *Mar. Pet. Geol.* 100, 165–178. <https://doi.org/10.1016/j.marpetgeo.2018.10.045>.
- Zhou, S., Xue, H., Ning, Y., Guo, W., Zhang, Q., 2018. Experimental study of supercritical methane adsorption in Longmaxi shale: insights into the density of adsorbed methane. *Fuel* 211, 140–148. <https://doi.org/10.1016/j.fuel.2017.09.065>.



- Zolfaghari, A., Dehghanpour, H., Holyk, J., 2017. Water sorption behaviour of gas shales: I. Role of clays. *Int. J. Coal Geol.* 179, 130–138. <https://doi.org/10.1016/j.coal.2017.05.008>.
- Zolfaghari, A., Dehghanpour, H., Xu, M., 2017. Water sorption behaviour of gas shales: II. Pore size distribution. *Int. J. Coal Geol.* 179, 187–195. <https://doi.org/10.1016/j.coal.2017.05.009>.
- Zou, J., Rezaee, R., Liu, K., 2017. Effect of temperature on methane adsorption in shale gas reservoirs. *Energy Fuels* 31 (11), 12081–12092. <https://doi.org/10.1021/acs.energyfuels.7b02639>.
- Zou, J., Rezaee, R., Xie, Q., You, L., Liu, K., Saeedi, A., 2018. Investigation of moisture effect on methane adsorption capacity of shale samples. *Fuel* 232, 323–332. <https://doi.org/10.1016/j.fuel.2018.05.167>.
- Zuber, M.D., Williamson, J.R., Hill, D.G., Sawyer, W.K., Frantz Jr., J.H., 2002. A comprehensive reservoir evaluation of a shale reservoir—the New Albany shale. In: Paper Presented at the SPE Annual Technical Conference and Exhibition.